

AD-A075 252

NAVAL POSTGRADUATE SCHOOL MONTEREY CA

F/G 13/13

THE INFLUENCE OF PLATFORM-CONDUCTOR GAPS ON THE DYNAMIC RESPONS--ETC(U)

MAY 78 L F POWERS

UNCLASSIFIED

NL

1 OF 1
AD
A075252



AD A075252

DDC FILE COPY

SECURITY CLASSIFICATION OF THIS PAGE (When Data Entered)

REPORT DOCUMENTATION PAGE		READ INSTRUCTIONS BEFORE COMPLETING FORM
1. REPORT NUMBER	2. GOVT ACCESSION NO.	3. RECIPIENT'S CATALOG NUMBER
4. TITLE (and Subtitle) THE INFLUENCE OF PLATFORM-CONDUCTOR GAPS ON THE DYNAMIC RESPONSE OF OFFSHORE PLATFORMS		5. TYPE OF REPORT & PERIOD COVERED THESIS
7. AUTHOR(s) POWERS, LYNN FREDERICK / Powers		6. PERFORMING ORG. REPORT NUMBER
9. PERFORMING ORGANIZATION NAME AND ADDRESS MASS. INST. OF TECHNOLOGY		8. CONTRACT OR GRANT NUMBER(s) 9. Master's thesis,
11. CONTROLLING OFFICE NAME AND ADDRESS Code 031 NAVAL POSTGRADUATE SCHOOL MONTEREY, CALIFORNIA, 93940		10. PROGRAM ELEMENT, PROJECT, TASK AREA & WORK UNIT NUMBERS
14. MONITORING AGENCY NAME & ADDRESS (if different from Controlling Office) LEVEL		12. REPORT DATE MAY 78
		13. NUMBER OF PAGES 88
		15. SECURITY CLASS. (of this report) UNCLASS
16. DISTRIBUTION STATEMENT (of this Report) APPROVED FOR PUBLIC RELEASE; DISTRIBUTION UNLIMITED		15a. DECLASSIFICATION/DOWNGRADING SCHEDULE
17. DISTRIBUTION STATEMENT (of the abstract entered in Block 20, if different from Report)		
18. SUPPLEMENTARY NOTES		
19. KEY WORDS (Continue on reverse side if necessary and identify by block number) OFFSHORE PLATFORMS, PLATFORM-CONDUCTOR GAPS, DYNAMIC RESPONSE		
20. ABSTRACT (Continue on reverse side if necessary and identify by block number) SEE REVERSE		

DD FORM 1473
1 JAN 73
(Page 1)

EDITION OF 1 NOV 68 IS OBSOLETE
S/N 0102-014-6601

UNCLASS

SECURITY CLASSIFICATION OF THIS PAGE (When Data Entered)

251 450

79 10 19 054

ABSTRACT

↘ The prerequisite to a dynamic analysis of an ocean platform is an accurate baseline measurement of the fundamental flexural and torsional natural frequencies. As an element of this baseline, the author uses the Runge-Kutta numerical integration method to determine the influence of a non-linear structural element on the measurement of the fundamental flexural natural frequency of the system. The non-linear phenomena which was investigated was the collision between the vertical conductor pipes and their guide collars on the platform. The analysis proved that for large excitation loads the response is non-linear, but that there is an excitation level below which the non-linearity is negligible.

Thesis Supervisor: Professor J. Kim Vandiver
Title : Assistant Professor of Ocean Engineering ↘

Approved for public release;
distribution unlimited.

THE INFLUENCE OF PLATFORM-CONDUCTOR GAPS ON THE
DYNAMIC RESPONSE OF OFFSHORE PLATFORMS

by

LYNN FREDERICK POWERS
B.S.E.E., PURDUE UNIVERSITY
(1971)

SUBMITTED IN PARTIAL FULFILLMENT
OF THE REQUIREMENTS FOR THE
DEGREE OF
OCEAN ENGINEER
AND THE DEGREE OF
MASTER OF SCIENCE IN
NAVAL ARCHITECTURE AND MARINE ENGINEERING
at the
MASSACHUSETTS INSTITUTE OF TECHNOLOGY
MAY 1978

© Lynn Frederick Powers

Signature of Author..... *Lynn F. Powers*.....
Department of Ocean Engineering
May 12, 1978
Certified by..... *J. Kim Vandiver*.....
Thesis Supervisor
Accepted by..... *A. Douglas Carmichael*.....
Chairman, Departmental
Committee on Graduate Students

THE INFLUENCE OF PLATFORM-CONDUCTOR GAPS ON THE
DYNAMIC RESPONSE OF OFFSHORE PLATFORMS

by

LYNN FREDERICK POWERS

Submitted to the Department of Ocean Engineering on
May 12, 1978 in partial fulfillment of the requirements for
the Degree of Ocean Engineer and the Degree of Master of
Science in Naval Architecture and Marine Engineering.

ABSTRACT

The prerequisite to a dynamic analysis of an ocean platform is an accurate baseline measurement of the fundamental flexural and torsional natural frequencies. As an element of this baseline, the author uses the Runge-Kutta numerical integration method to determine the influence of a non-linear structural element on the measurement of the fundamental flexural natural frequency of the system. The non-linear phenomena which was investigated was the collision between the vertical conductor pipes and their guide collars on the platform. The analysis proved that for large excitation loads the response is non-linear, but that there is an excitation level below which the non-linearity is negligible.

Thesis Supervisor: Professor J. Kim Vandiver
Title : Assistant Professor of Ocean Engineering

ACKNOWLEDGEMENTS

The author wishes to express his sincere gratitude to Professor J. Kim Vandiver for his unfailing support and constructive guidance throughout the completion of this thesis.

A special thank you goes to Mary Ellen White who, although completely unfamiliar with a thesis format, cheerfully and expeditiously produced a professional report.

I am indebted to my wife, Beverly, and to my children who have sacrificed much in order that I might complete my studies at M.I.T.

This thesis is dedicated to my late father, Maynard H. Powers, whose memory remains a daily inspiration.

Accession For	
NTIS GAMA	<input checked="checked" type="checkbox"/>
DDC TAB	<input type="checkbox"/>
Unannounced	<input type="checkbox"/>
Justification	
By _____	
Distribution/	
Availability Codes	
Dist	Avail and/or special
A	

Table of Contents

Title page	1
Abstract	2
Acknowledgements	3
Table of Contents	4
List of Figures	5
List of Tables	6
Chapter 1. Problem Definition and Model Description	7
Chapter 2. Non-dimensionalization of the System	
Equations of Motion	14
Chapter 3. Method of Solution and Error Analysis	15
Chapter 4. Analysis Results	22
Bibliography	38
Appendix A	A-1
Appendix B	B-1

List of Figures

<u>Figure</u>	<u>Title</u>	<u>Page</u>
1.1	System Schematic Diagram	9
1.2	Contact Force Components	12
4.1	Platform Displacement vs. γ_1	24
4.0	Platform Response for $F_{01} = 0.001$; $\gamma_1 = 0.5$	25
4.01	Fourier Transform of Platform Response for $F_{01} = 0.001$; $\gamma_1 = 0.5$	26
4.2	$ R(\omega) $ vs. γ^* ; $\gamma_1 = 0.5$	28
4.3	$ R(\omega) $ vs. γ^* ; $\gamma_1 = 0.8$	29
4.4	$ R(\omega) $ vs. γ^* ; $\gamma_1 = 1.0$	30
4.5	$ R(\omega) $ vs. γ^* ; $\gamma_1 = 1.5$	31
4.6	$ R(\omega) $ vs. γ^* ; $\gamma_1 = 2.0$	32
4.7	$ R(\omega) $ vs. γ^* ; $\gamma_1 = 3.0$	33
4.8	$ R(\omega) $ vs. γ^* ; $\gamma_1 = 5.0$	34
B.1	Platform Response for $F_{01} = 0.01$; $\gamma_1 = 0.5$	B-3
B.2	Platform Response for $F_{01} = 0.01$; $\gamma_1 = 0.8$	B-4
B.3	Platform Response for $F_{01} = 0.01$; $\gamma_1 = 1.0$	B-5
B.4	Platform Response for $F_{01} = 0.01$; $\gamma_1 = 1.5$	B-7
B.5	Platform Response for $F_{01} = 0.01$; $\gamma_1 = 2.0$	B-9
B.6	Platform Response for $F_{01} = 0.01$; $\gamma_1 = 3.0$	B-10
B.7	Platform Response for $F_{01} = 0.01$; $\gamma_1 = 5.0$	B-11
B.8	Platform Response for $F_{01} = 0.001$; $\gamma_1 = 0.5$	B-13
B.9	Platform Response for $F_{01} = 0.001$; $\gamma_1 = 0.8$	B-14
B.10	Platform Response for $F_{01} = 0.001$; $\gamma_1 = 1.0$	B-15

List of Figures, continued

<u>Figure</u>	<u>Title</u>	<u>Page</u>
B.11	Platform Response for $F_{01} = 0.001$; $\gamma_1 = 1.5$	B-16
B.12	Platform Response for $F_{01} = 0.001$; $\gamma_1 = 2.0$	B-17
B.13	Platform Response for $F_{01} = 0.001$; $\gamma_1 = 3.0$	B-19
B.14	Platform Response for $F_{01} = 0.001$; $\gamma_1 = 5.0$	B-21
B.15	Platform Response for $F_{01} = 0.0001$; $\gamma_1 = 0.5$	B-22
B.16	Platform Response for $F_{01} = 0.0001$; $\gamma_1 = 0.8$	B-23
B.17	Platform Response for $F_{01} = 0.0001$; $\gamma_1 = 1.0$	B-24
B.18	Platform Response for $F_{01} = 0.0001$; $\gamma_1 = 1.5$	B-25
B.19	Platform Response for $F_{01} = 0.0001$; $\gamma_1 = 2.0$	B-26
B.20	Platform Response for $F_{01} = 0.0001$; $\gamma_1 = 3.0$	B-27
B.21	Platform Response for $F_{01} = 0.0001$; $\gamma_1 = 5.0$	B-28

List of Tables

<u>Table</u>	<u>Title</u>	<u>Page</u>
2.1	Summary of Non-dimensional Parameters	15
4.1	System Parameter Values	23
B.1	Computer Run Code Summary	B-1

CHAPTER 1

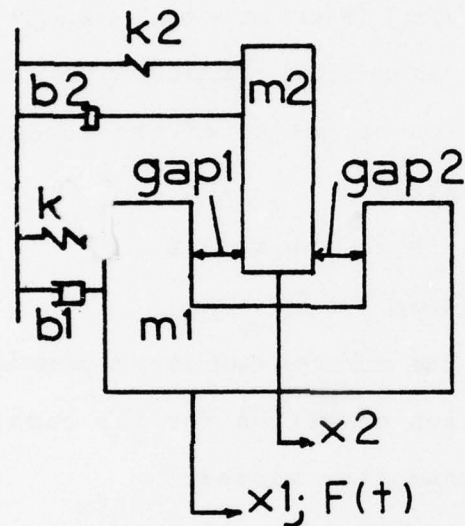
Problem Definition and Model Description

The size of an ocean platform and the variation of environmental excitations on it make the determination of the integrity of the platform a vital concern to the ocean engineer. A method of integrity certification which is under development utilizes on-location measurement of the platform natural frequencies to determine if a structural failure has occurred. This technique requires an initial, accurate baseline determination of the platform natural frequencies. These baseline measurements will be compared to values obtained at later dates to establish if any changes have occurred. However, before a shift in natural frequency can be related to damage, all other sources of change, such as live platform load variations and marine growth, must be evaluated. In this paper, the author addresses the impact of a non-linear structural dynamic element on the measurement of the fundamental natural frequency.

For example purposes, the platform to be analyzed is a deep ocean drilling platform with a centrally located, unattached, conductor which extends from the platform deck to the ocean floor. The purpose of the analysis is to determine the effect of the non-linear interaction between the platform and the conductor on the measured natural frequency of the entire system in the fundamental flexural mode. In order to limit the problem to a manageable size,

several constraints must be placed on the system. Principal among these is the use of a periodic excitation to drive the system. This constraint simplifies the identification of the platform response frequencies. Secondly, the initial separation between the platform and the conductor is set to zero. In the author's opinion, this position presents a worst case condition, and it is also the most likely from engineering considerations of the conductor installation. The excitation loads were varied in order to demonstrate a breakpoint between the linear and non-linear behavior of the structure. The remaining system parameters were set equal to specific values based on engineering judgement and the best information available. The greatest uncertainty in parameter estimation occurred in the determination of the conductor parameters. A more definitive investigation of these quantities should be performed before further system analysis is conducted.

The platform can be modeled as a mass, spring and damper system which surrounds another mass, spring and damper system modeling the conductor. The platform mass is free to move along its horizontal axis, and if sufficient excitation is provided, collide with the conductor mass. This collision causes a reduction in the platform movement while increasing the motion of the conductor. The figure on the next page illustrates the model.



- m_1 platform mass
- k_1 platform spring constant
- b_1 platform viscous damping coefficient
- m_2 conductor mass
- k_2 conductor spring constant
- b_2 conductor viscous damping coefficient
- x_1 platform displacement from equilibrium position
- x_2 conductor displacement from equilibrium position

FIGURE 1.1 SYSTEM SCHEMATIC DIAGRAM

A mathematical solution for the response of the model is derived in the following manner:

1. Equation of motion of the platform moving separately:

$$m_1 \ddot{x}_1 + b_1 \dot{x}_1 + k_1 x_1 = F \sin \omega t,$$

or,
$$\ddot{x}_1 = (1/m_1) (F \sin \omega t - b_1 \dot{x}_1 - k_1 x_1) \quad (1)$$

where x_1 is relative to the unforced equilibrium position of the platform.

2. Equation of motion of the conductor moving separately:

$$m_2 \ddot{x}_2 + b_2 \dot{x}_2 + k_2 x_2 = 0$$

or,
$$\ddot{x}_2 = (1/m_2) (-b_2 \dot{x}_2 - k_2 x_2) \quad (2)$$

where x_2 is relative to the unforced equilibrium position of the conductor.

3. Equation of motion for the combined platform and conductor masses:

$$(m_1 + m_2) \ddot{x}_1 + b_1 \dot{x}_1 + b_2 \dot{x}_1 + k_1 x_1 + k_2 x_2 = F \sin \omega t$$

or,
$$\ddot{x}_1 = (1/m_1 + m_2) (F \sin \omega t - (b_1 + b_2) \dot{x}_1 - k_1 x_1 - k_2 x_2) \quad (3)$$

In equations 1, 2 and 3, masses, damping constants and spring constants are denoted by m , b and k respectively. Subscript 1 designates the platform and subscript 2 denotes the conductor. Equations 1 and 2 completely describe the ~~response of the system when the platform and conductor are~~ in motion separately. Equation 3 describes the response after a collision has occurred. However, several questions about the system have yet to be answered. Specifically, what happens at the time of collision, how is the time of collision determined, and how is the time of separation

determined? The answers to these questions provide the remaining equations which will define the motion of the platform/conductor system at all times.

To determine when a collision occurs, the gaps between the platform and the conductor must be continuously determined. When the value of the gap distance on either side of the conductor goes to zero, a collision has occurred. The following equation defines this feature mathematically.

4. Total gap distance:

$$\text{gap}_1 + \text{gap}_2 = d_o - d_i \quad (4)$$

where d_o is the platform aperture diameter and d_i is the conductor outside diameter.

5. Gap distance at any time, t :

$$\begin{aligned} \text{gap}_1(t) = \text{gap}_1(t-1) + (x_2(t) - x_2(t-1)) - (x_1(t) \\ - x_1(t-1)) \end{aligned} \quad (5a)$$

$$\text{gap}_2(t) = d_o - d_i - \text{gap}_1(t) \quad (5b)$$

where $(t-1)$ defines the time increment just prior to the time, t , being calculated.

At the time of collision, energy will be lost. However, momentum is conserved. Therefore the velocity of the system can be determined as shown below.

6. Conservation of momentum:

$$m_1 \dot{x}_1 = (m_1 + m_2) \dot{x}$$

or, $\dot{x} = (m_1 / (m_1 + m_2)) \dot{x}_1$ (6)

Since both the conductor and platform are moving at the same velocity, the value of \dot{x} is the value of \dot{x}_1 in equation 3.

Finally, an equation is needed to determine if the platform and conductor have separated. The contact force can be used to perform this determination. The diagram below illustrates the contact force, $f(t)$.

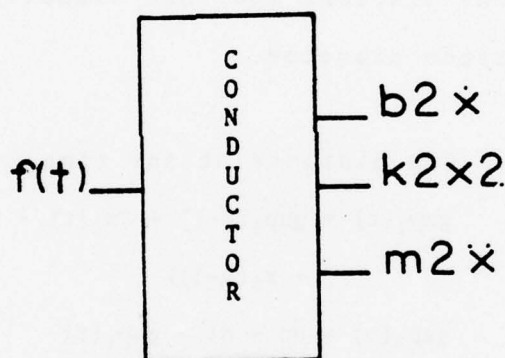


FIGURE 1.2 CONTACT FORCE COMPONENTS

7. Contact force:

$$f(t) = b_2 \dot{x} + k_2 x_2 - m_2 \ddot{x} \quad (7)$$

In summary, the ocean platform has been modeled and the mathematical equations have been written to define the motion of the platform system at any point in time. The next chapter illustrates the process of non-dimensionalizing these equations which will lend them to analysis on a more general level. A numerical integration method of solution will then be presented after which the results of the analysis will be determined.

CHAPTER 2

Non-dimensionalization of the System Equations of Motion

The removal of dimensions from the system equations of motion performs two important functions. First, the dimensionless parameters of the system have a greater application. Secondly, systematic variation of the dimensionless parameters will provide data which can be compared to known standards when the excitation is periodic.

Eighteen parameters are contained in equations 1 through 6 in chapter 1. The equations can be non-dimensionalized by proper selection of reference quantities for length, mass and time. The author defines F/k_1 , m_1 and $2\pi/\omega_{01}$ as the reference quantities for length, mass and time respectively. The variables in equations 1 through 6 for displacement, velocity, acceleration, total gap distance and time are made dimensionless by division and differentiation using these reference values. The conductor parameters of mass, viscous damping coefficient and spring constant are non-dimensionalized by dividing by the respective platform parameters. After substitution of the new variables into equations 1, 2, 3 and 7, the damping coefficient of the platform is divided by product of two times m_1 times ω_{01} . This ratio is defined as the damping factor, ζ_1 , and is dimensionless. The contact force variable becomes dimensionless after all the parameters of equation 7 have been non-dimensionalized.

For clarity, the contact force variable is redefined \hat{F} to identify it as dimensionless. The remaining parameter, excitation frequency, is nondimensionalized by dividing by the platform natural frequency. The dimensionless parameters are summarized in Table 2.1.

Table 2.1, Summary of Non-Dimensional Parameters

Non-dimensional Variable	Dimensional Ratio
r	$x_1/(F/k_1)$
c	$x_2/(F/k_1)$
τ	$t/(2\pi/\omega_{01})^*$
ρ	k_2/k_1
μ	m_2/m_1
ψ	b_2/b_1
ζ_1	$b_1/2m_1\omega_{01}$
γ_1	ω/ω_{01}
$d\tilde{r}$	$1/(F/k_1) d\tilde{x}_1$
d^2r	$1/(F/k_1) d^2x_1$
$d\tilde{c}$	$1/(F/k_1) dx_2$
d^2c	$1/(F/k_1) d^2x_2$
$d\tau$	$1/(2\pi/\omega_{01}) dt$
$d\tau^2$	$1/(4\pi^2/\omega_{01}^2) dt^2$
\hat{F}	F/m_1g
\bar{D}	$(d_o - d_i)/(F/k_1)$

* $\omega_{01} = (k_1/m_1)^{1/2}$

The equations of motion from chapter 1 and their dimensionless equivalents are presented on the following pages.

1. Platform motion moving separately:

$$\ddot{x}_1 = (1/m_1) (F \sin \omega t - b_1 \dot{x}_1 - k_1 x_1) \quad (1)$$

NON-DIMENSIONALIZED

$$\ddot{r} = 4\pi^2 (\sin 2\pi\gamma_1 \tau - r) - 4\pi\zeta_1 \dot{r} \quad (1.1)$$

2. Conductor motion moving separately:

$$\ddot{x}_2 = (1/m_2) (-b_2 \dot{x}_2 - k_2 x_2) \quad (2)$$

NON-DIMENSIONALIZED

$$\ddot{c} = (1/\mu) (4\pi\psi\zeta_1 \dot{c} - 4\pi^2 \rho c) \quad (2.1)$$

3. Combined platform / conductor motion:

$$\ddot{x}_1 = (1/m_1+m_2) (F \sin \omega t - (b_1+b_2)\dot{x}_1 - k_1 x_1 - k_2 x_2) \quad (3)$$

NON-DIMENSIONALIZED

$$\ddot{r} = (1/(1+\mu)) (4\pi^2 (\sin 2\pi\gamma_1 \tau - r - \rho c) - 4\pi(\zeta_1 \dot{r} + \psi\zeta_1 \dot{r})) \quad (3.1)$$

4. Gap distances at any time, t:

$$\begin{aligned} \text{gap}_1(t) &= \text{gap}_1(t-1) + (x_2(t) - x_2(t-1)) - \\ &\quad (x_1(t) - x_1(t-1)) \end{aligned} \quad (5a)$$

$$\text{gap}_2(t) = d_0 - d_i - \text{gap}_1(t) \quad (5b)$$

NON-DIMENSIONALIZED

$$\begin{aligned} \overline{\text{gap}}_1(\tau) &= \overline{\text{gap}}_1(\tau-1) + (c(\tau) - c(\tau-1)) - \\ &\quad (r(\tau) - r(\tau-1)) \end{aligned} \quad (5a.1)$$

$$\overline{\text{gap}}_2(\tau) = \overline{D} - \overline{\text{gap}}_1(\tau) \quad (5b.1)$$

5. Conservation of momentum:

$$\dot{x} = (m_1/m_1 + m_1) \dot{x}_1 \quad (6)$$

NON-DIMENSIONALIZED

$$\dot{r} = (1/(1 + \mu)) \dot{r} \quad (6.1)$$

Equation 6.1 appears inconsistent. However, it should be interpreted as the velocity the moment after a collision is equal to a constant times the value of the velocity just before the collision.

7. Contact Force

$$f(t) = b_2 \dot{x} + k_2 x_2 - m_2 \ddot{x} \quad (7)$$

Non-dimensionalized

$$\hat{f} = \psi \zeta_1 \dot{\hat{x}} + \rho c - (1/4\pi^2) \mu \ddot{\hat{x}} \quad (7.1)$$

The equations of motion describing the platform/conductor system have been non-dimensionalized and are in a form which lends then to analysis through the use of an integrative method of solution.

CHAPTER 3

Method of Solution and Error Analysis

Since the interaction between the platform and the conductor are quite non-linear, analytic methods of solution must be bypassed for numerical means. Of these, the Runge-Kutta (R-K) is most fitting for this analysis because the method is self-starting and easily adaptable to computer programming.

Classically, the R-K method expresses the difference between the values of y at $x(n+1)$ and $x(n)$, where $x(n+1)$ and $x(n)$ are $(n+1)$ and (n) increments of x away from a reference point x_0 , if the increments are constant as they will be for this analysis. Mathematically this statement becomes:

$$y(n+1) - y(n) = \sum_{i=1}^m a_i k_i \quad (8)$$

where the a_i 's are constant, the k_i 's are determined by Taylor series expansion and 'm' is the order of the R-K method being used. cursory examination of equation 8 indicates that higher orders of the R-K method yield a greater number of terms for each value of $y(n+1)$. It is to be shown that higher orders also yield greater accuracy.

The principle error in the Runge-Kutta method is the truncation error which is defined:

$$T_m = c(h)^{m+1} + o(h)^{m+2}$$

where: m is the order of the R-K method

h is the increment $(x_1 - x_0)$

c is a constant of $d^{m+1}f/dx^{m+1}$.

The order of the h^{m+2} term is generally smaller than the h^{m+1} term and will not be considered further. The truncation error for any term may be defined:

$$T_i \propto h^{m+1} \cdot (\text{number of steps}),$$

where $(\text{number of steps}) = \text{constant}/h$.

Therefore,

$$T_i \propto h^m$$

An estimation of the magnitude of the truncation error for a term can be determined by comparison of the integration values using spacing increments of h and $2h$.

$$T_m = y(x_i) - y_i^{(2h)} = c(2h)^m = c(h)^m 2^m$$

$$T_m = y(x_i) - y_i^{(h)} = c(h)^m,$$

where $(2h)$ and (h) distinguish between integration increment values. Subtraction of the second equation from the first yields:

$$y_i^{(h)} - y_i^{(2h)} = c(h)^m (2^m - 1) \text{ or,}$$

$$T_m = (y_i^{(h)} - y_i^{(2h)}) / (2^m - 1).$$

After actual calculation, $T_m = 0.0\dots b$, where b is the m^{th} decimal place.

Keying on minimizing truncation error, the author selected a fourth order Runge-Kutta method for use in this paper. The numerical approximation equations for this method are as

follows:

$$y(n+1) - y(n) = \frac{1}{6} (k_1 + 2k_2 + 2k_3 + k_4)$$

$$k_1 = h f(x(n), y(n))$$

$$k_2 = h f(x(n) + \frac{1}{2}h, y(n) + \frac{1}{2}k_1)$$

$$k_3 = h f(x(n) + \frac{1}{2}h, y(n) + \frac{1}{2}k_2)$$

$$k_4 = h f(x(n) + h, y(n) + k_3)$$

To perform the R-K integration for the determination of the platform and conductor displacements, it is necessary to transform the second order differential equations of chapter 2 into first order differential equations. This elementary procedure yields the equations shown below.

Platform Displacement (moving separately)

$$r_1 = r$$

$$\dot{r}_1 = r_2$$

$$\dot{r}_2 = \ddot{r}$$

$$\dot{r}_2 = 4\pi^2 (\sin 2\pi \tau - r_1) - 4\pi\zeta_1 r_2 \quad (1.2)$$

$$\dot{r}_1 = r_2 \quad (1.3)$$

Conductor Displacement (moving separately)

$$c_1 = c$$

$$\dot{c}_1 = c_2$$

$$\dot{c}_2 = \ddot{c}$$

$$\dot{c}_2 = (1/\mu) (4\pi\psi\zeta_1 c_2 - 4\pi^2 \rho c_1) \quad (2.2)$$

$$\dot{c}_1 = c_2 \quad (2.3)$$

Combined Platform/Conductor Displacement

$$\begin{aligned} \ddot{f}_2 = & (1/1+\mu) (4\pi^2(\sin 2\pi\gamma_1\tau - r_1 - \rho c_1) \\ & - 4\pi(\zeta_1 r_2 + \psi \zeta_1 r_2)) \end{aligned} \quad (3.2)$$

$$\dot{r}_1 = r_2 \quad (3.3)$$

Platform/Conductor Gap

$$\begin{aligned} \overline{\text{gap}}_1(\tau) = & \overline{\text{gap}}_1(\tau-1) + (c_1(\tau) - c_1(\tau-1)) \\ & - (r_1(\tau) - r_1(\tau-1)) \end{aligned} \quad (5a.2)$$

Contact Force

$$\hat{f} = \psi \zeta_1 r_1 + \rho c_1 - (1/4\pi^2)\mu r_2 \quad (7.2)$$

The computer program utilized in this paper was designed and written by the author. A description, user's guide and a printout of the program with output are presented in Appendix A.

CHAPTER 4

Analysis Results

As it was mentioned in chapter 1, the problem has been constrained to maintain manageability. As the first iteration toward understanding the response characteristics of the platform system, the author set the dimensionless ratios of the conductor to platform mass, viscous damping coefficient and spring constant to constant values. The damping factor, ζ_1 , and the total gap distance were also made equal to constants. The excitation force parameter, F_{01} , was given three discrete values for the purpose described in chapter 1. The ratio of excitation frequency to platform natural frequency, γ_1 , was given a range of seven values from 0.5 to 5.0. This range yields a summary plot of the platform displacement which is similar in appearance to a standard transfer function plot. The values of the platform mass and natural frequency were estimated from previous platform analysis experience. The damping factor was also determined in this manner. With the values for natural frequency and mass, the platform spring constant was calculated. The ratios between conductor and platform parameters were then estimated. Using these percentages, the values of conductor mass, viscous damping coefficient and spring constant were calculated. The values of the system parameters are listed in Table 4.1.

TABLE 4.1, System Parameter Values

<u>Parameter</u>	<u>Value</u>
ψ	0.009998
ζ	0.03
μ	0.1
γ_1	0.5, 0.8, 1.0, 1.5, 2.0, 3.0, 5.0
ρ	0.01
F01	0.01, 0.001, 0.0001
m_1	2.07×10^4 (lb-sec ²)/inch
m_2	2.07×10^3 (lb-sec ²)/inch
b_1	3.12×10^4 (lb-sec)/ft
b_2	3.124×10^3 (lb-sec)/ft
k_1	9.08×10^4 lb/in
k_2	9.08×10^2 lb/in
ω_{01}	2.09 radians/second
ω_{02}	0.628 radians/second
d_o	19.5 inches
d_i	17.2 inches

The system was analyzed for the platform response over the range of γ_1 for each excitation force.

The output of the computer program was two plots. Each plot was coded on the abscissa to denote the type of response that was plotted and the specific values of γ_1 and F01 used for that computer run. A complete description of the coding and the individual displacement vs. τ plots for the twenty-one parameter combinations are presented with their analyses in Appendix B. Each analysis discusses the effect of the excitation frequency on the response frequency, the dynamic equilibrium position either positive or negative of the static equilibrium zero position, the steady-state magnitude of the response and the primary response frequencies.

As an example, if γ_1 and F01 were set to values of

0.5 and 0.001 respectively, the resulting platform displacement and fourier transform are shown in Figures 4.0 and 4.01. The platform response has a period of 2π which is the period of the excitation frequency, 1 radian/second. The dynamic equilibrium position is slightly negative. The Fourier transform yields two frequencies, the excitation frequency and the platform natural frequency.

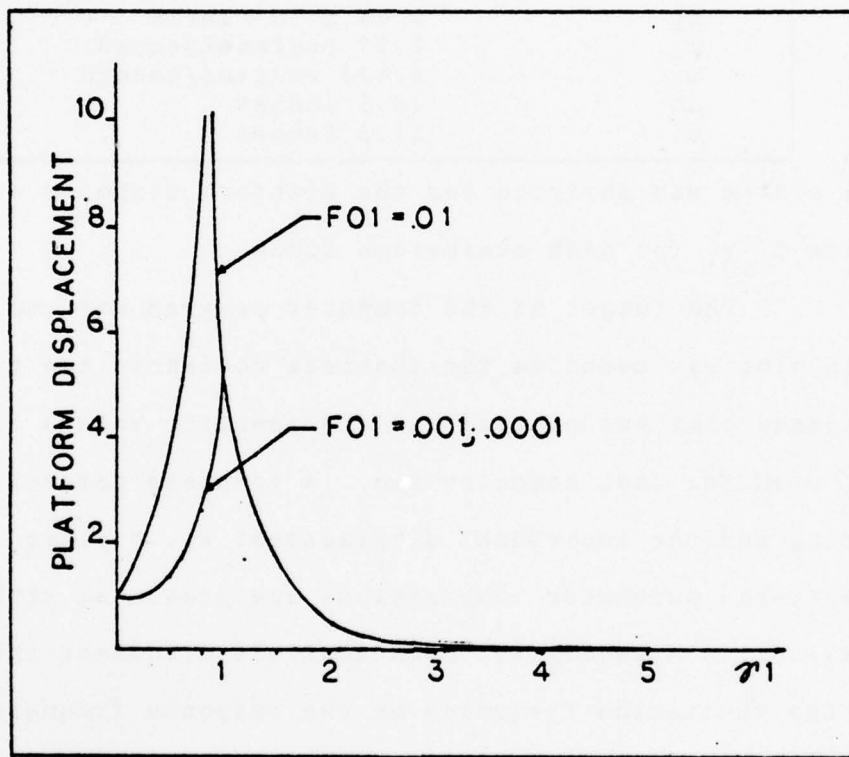


Figure 4.1, Platform Displacement vs. γ_1

In Figure 4.1 the dimensionless platform displacement is plotted against the ratio of excitation frequency to platform natural frequency, γ_1 . The non-linearity of the

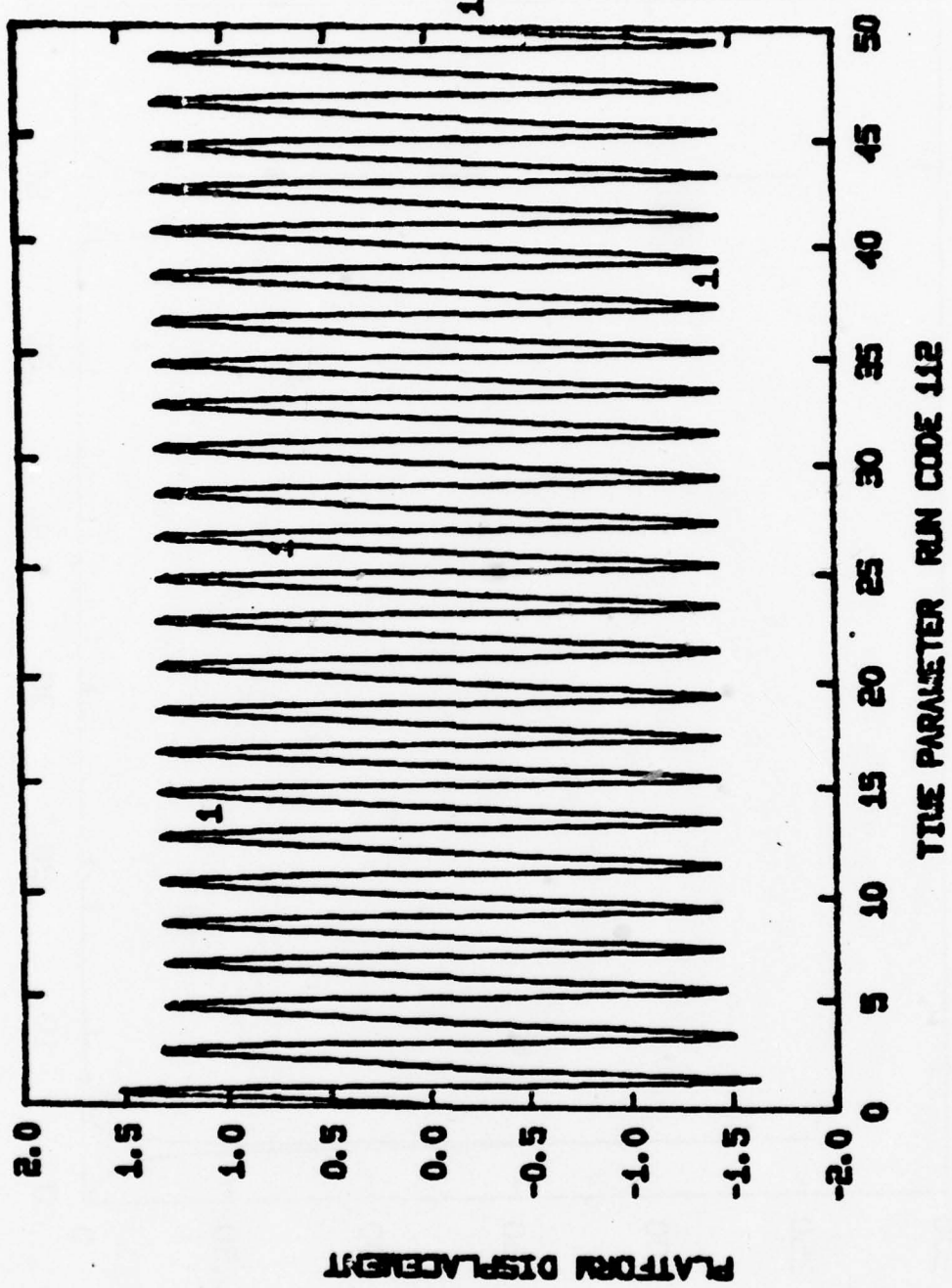


Figure 4.0

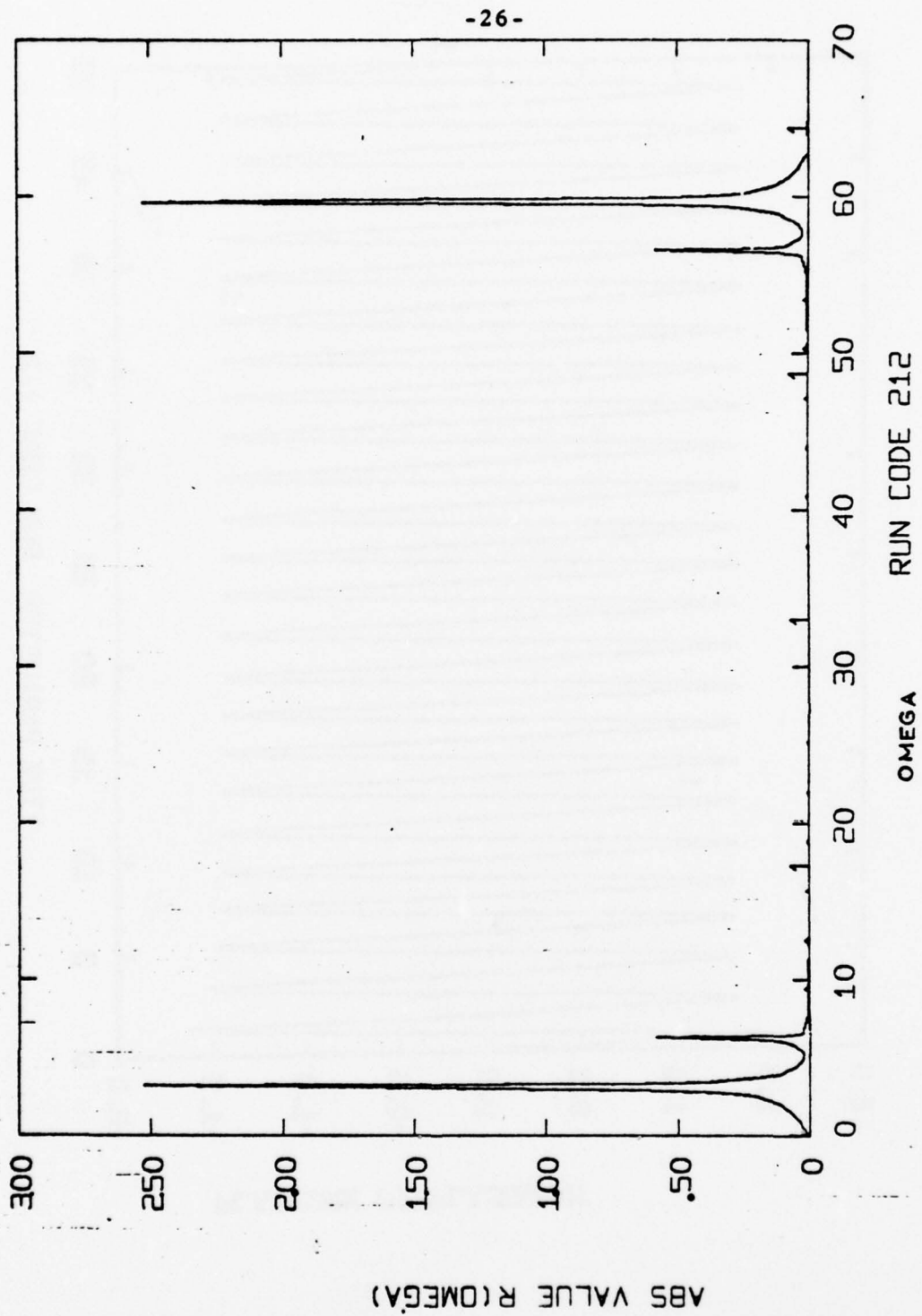


Figure 4.01

system is demonstrated by the reduction in magnitude as the excitation force is decreased from 0.01 to 0.001. The decrease has also produced a frequency shift in the platform response to the right. The coincidental displacement plots for the excitation force equal to 0.001 and 0.0001 imply that the system is linear for these load levels. Thus, there is a breakpoint in the excitation force level below which the non-linear influence of the conductor on the platform natural frequency is negligible. However, the non-linearity has reduced the magnitude of the response.

On the following pages, Figures 4.2 through 4.8 present plots of the absolute value of the Fourier transform of the platform displacement against the ratio of response frequency to the platform natural frequency which has been designated γ^* . Each figure displays the displacement magnitudes for a specific value of the ratio of excitation frequency to platform natural frequency, γ_1 . The congruency of the plots for F01 equal to 0.001 and 0.0001 over all values of γ_1 reinforces the statements made previously concerning the non-linear effect of the conductor.

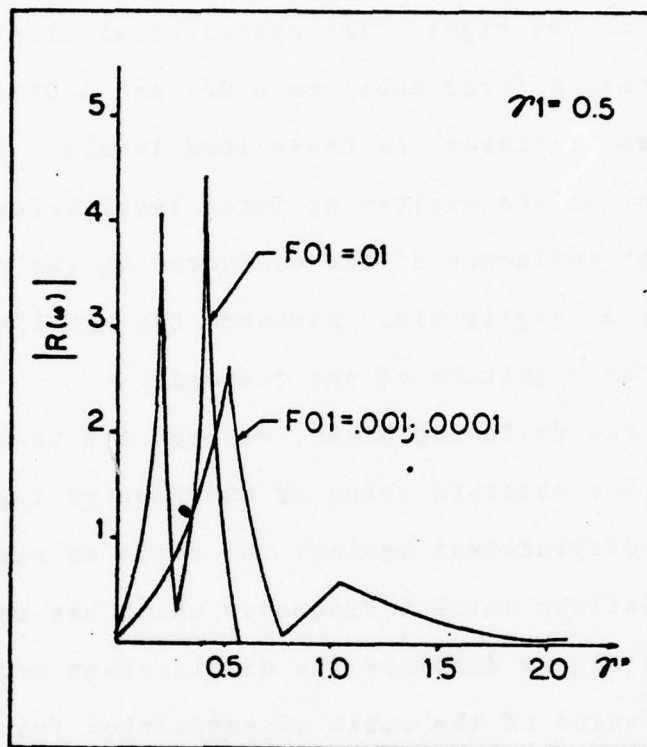


Figure 4.2, $|R(\omega)|$ vs. γ^* ; $\gamma_1 = 0.5$

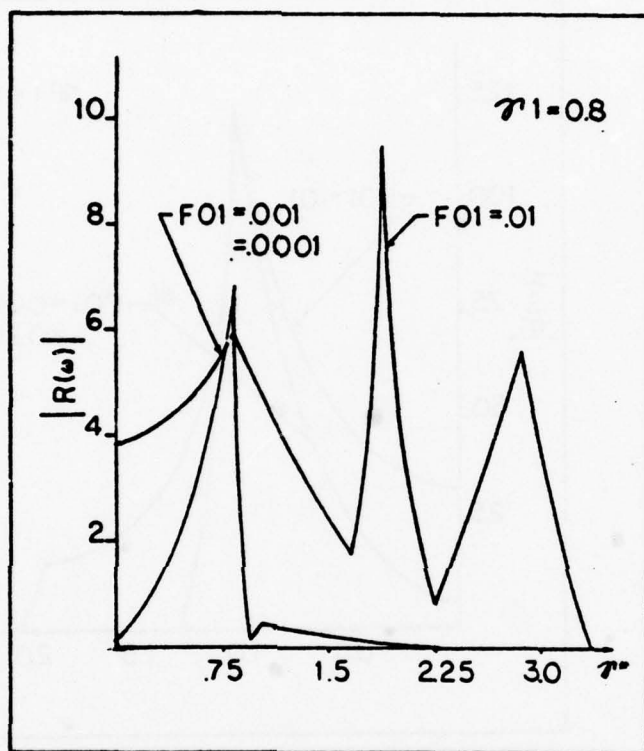


Figure 4.3, $|R(\omega)|$ vs. γ^* ; $\gamma_1 = 0.8$

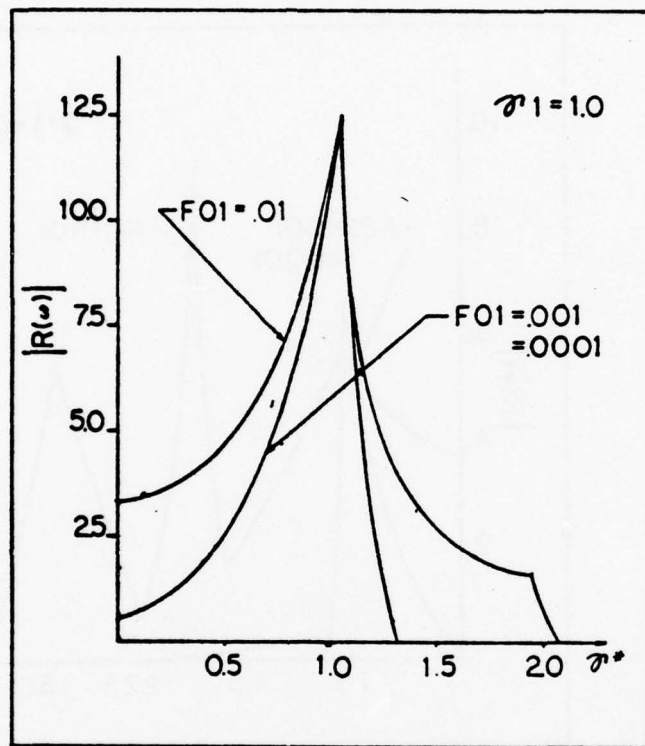


Figure 4.4, $|R(\omega)|$ vs. γ^* ; $\gamma_1 = 1.0$

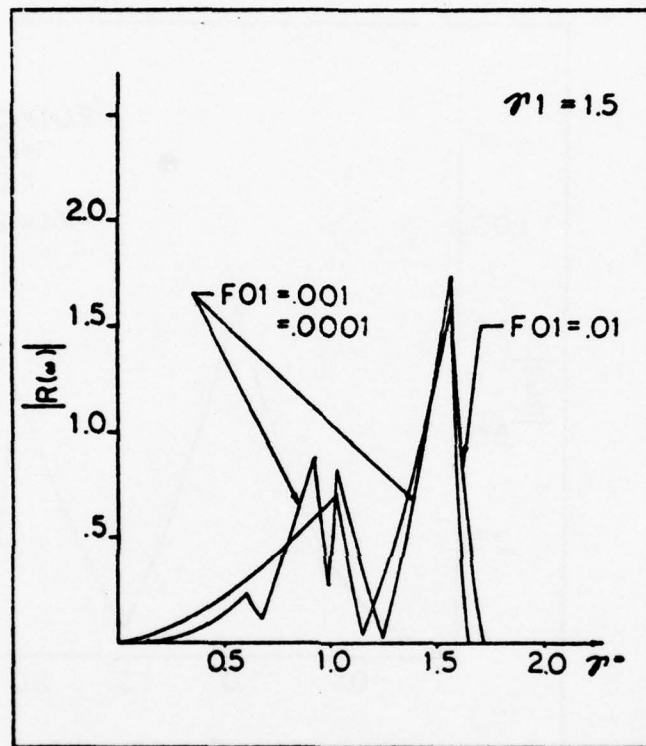


Figure 4.5, $|R(\omega)|$ vs. γ^* ; $\gamma_1 = 1.5$

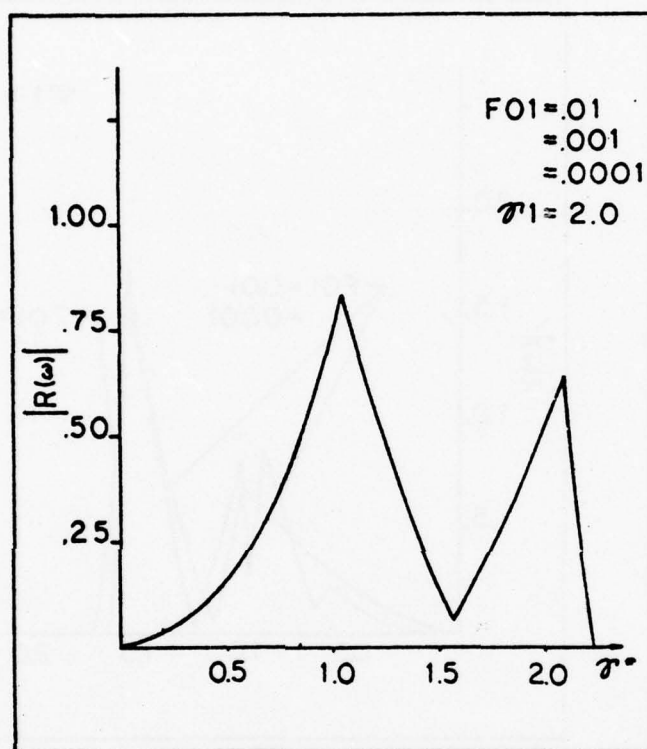


Figure 4.6, $|R(\omega)|$ vs. γ^* ; $\gamma_1 = 2.0$

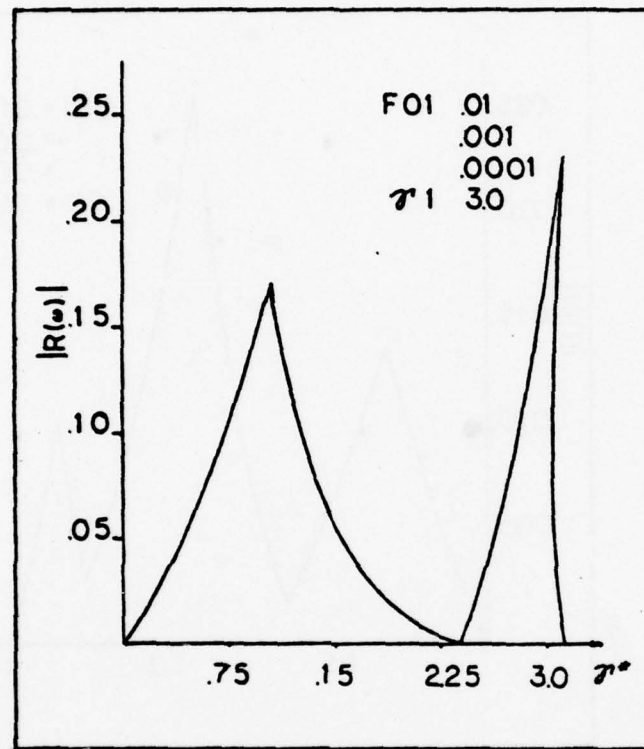


Figure 4.7, $|R(\omega)|$ vs. γ^* ; $\gamma_1 = 3.0$

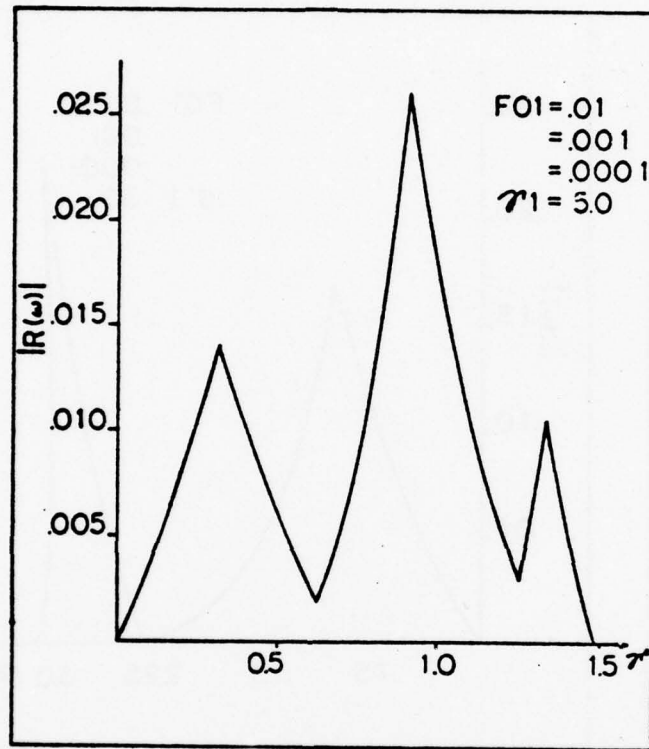


Figure 4.8, $|R(\omega)|$ vs. γ^* ; $\gamma_1 = 5.0$

Principally, the analysis has shown that for large values of excitation force the system is non-linear. This is clearly displayed by the shift in the platform natural frequency. If the excitation load is below an as yet undetermined level, the natural frequency of the platform is unaffected by the non-linear influence of the conductor. However, the non-linearity reduces the steady-state platform magnitude. The analysis consistently attributes the response frequency of the platform to a function of excitation frequency and the platform natural frequency. Normally, the platform would respond at the excitation frequency in the steady-state mode. However, the analysis was conducted by numerical integration until steady-state was attained. Therefore, when the Fourier transform of the platform displacement was taken, the transient effects of the problem "start-up" were included and presented in the transform results. This transform is more desirable than a pure steady-state transform since actual measurements on the platform are taken during random excitation and the transient effects will not have an opportunity to die out.

With the dimensionless excitation force equal to 0.01, the dynamic equilibrium of the system shifted markedly negative if the excitation frequency was near the platform natural frequency. At frequencies above the platform natural frequency, the dynamic equilibrium always shifted positively, but the shift was nearly indistinguishable. The dynamic

equilibrium position shift was inconsistent when the excitation frequency equalled the platform natural frequency. The period of the maximum platform displacement in steady-state was coincidental with the excitation period throughout the analysis. No further conclusions can be drawn from the data.

The Runge-Kutta numerical integration method has been an effective means of determining the dynamic characteristics of the system. It is evident that this analysis has raised more questions than it has answered because of the imposed parameter constraints. Even with these limitations, if several more of the parameters, i.e., the platform damping factor and the conductor/platform ratios were varied, the system response characteristics could be more accurately determined. The system should then be analyzed using an excitation approximating the environmental conditions to which the platform will be subjected to determine the fundamental flexural baseline response.

The computer program has some minor problems which could be eliminated for greater efficiency. The program was designed to analyze the system with one set of parameter values per computer run. However, it would be more economical to have the capability to increment those parameters chosen for variation over a set of values. This improvement would keep the program on the computer until all of the variations had been completed. The Runge-Kutta section of the program,

although correct and complete, does not allow for varying the incrementing variable. If the difference between two adjacent, integrated values of a variable reaches a magnitude that is too large, the program may overflow the computer memory capacity and generate output which contains only error messages. The author endured this perennial set-back because of the input requirements of the Fourier transform and plotting subroutines.

BIBLIOGRAPHY

1. Meirovitch, I., "Elements of Vibration Analysis," McGraw-Hill 1975, Chapters 1 and 2
2. Vandiver, J. K., "Dynamic Analysis of a Launch and Recovery System for a Deep Submersible," Unpublished Manuscript, pp 15 - 18
3. Ralston, A., "A First Course in Numerical Analysis," McGraw-Hill 1956, pp 191-201
4. Shearer, J. L., Murphy, A. T., Richardson, H. H., "Introduction to System Dynamics," Addison-Wesley 1971, Chapter 15.

APPENDIX A

The computer program was written to utilize a 4th order Runge-Kutta (R-K) numerical integration approximation for determining the dimensionless displacement of an ocean platform with a centrally located conductor. The values of the displacement are then printed out, plotted as a function of τ and subjected to a Fourier transform subroutine whose output absolute values are plotted as a function of the ω determined in the transform. Because the equations of the program are non-dimensionalized, the values of ω used for the Fourier transform plot are a function of τ , not real time, t . To convert ω (fourier transform) to an ω (real time), one must divide the product of ω (fourier transform) times ω (platform natural frequency) by 2π . The program has been designed to compute the platform response for one set of input parameter values per program execution. Thus, if γ_1 were assigned a range of values, the user must run the program on the computer once for each value of γ_1 .

The program is initiated by setting the arrays for the platform displacement and velocity, the conductor displacement and velocity, the gap values and time equal to zero. This step is followed by individually setting the values for the dimensionless parameters. The values of the dimensional parameters for excitation force, platform spring constant, platform aperture diameter and the conductor outside diameter

are then entered into the computer to calculate the value of the dimensionless total gap distance. The final initial conditions are input when the individual gap distances are set and the program begins execution.

The analysis begins by computing the first integration values of platform displacement and velocity, and the conductor displacement and velocity using the 'masses separated' R-K integration equations. Gap_1 is then calculated by subtracting the net change in platform displacement from the net change in the conductor displacement and adding this result to the old value of gap_1 . This new gap_1 is subtracted from the total gap distance to determine the new gap_2 . Gap_1 and gap_2 are checked for a zero or negative value indicating a collision between the platform and the conductor. If no collision has occurred, time is incremented and the integration takes place again. If there has been a collision, the value of the conductor velocity is changed to equal a new value of the platform velocity which is determined by conservation of momentum. The contact force between the platform and the conductor is checked for a zero or negative value. If the contact force is zero or negative, the program returns to the 'masses separated' R-K integration. If the contact force is greater than zero, the program executes the R-K approximation using the equations of motion for the combined masses. The program again checks for a zero contact force and increments

the R-K approximations for separated or combined masses as the situation dictates until the limit of the increment count is reached.

At this time the platform displacement is transferred into a plotting subroutine for a pictorial display of the result. The platform displacement array is then transformed into a complex number array and transferred to the Fourier transform subroutine(FFT). The output of the FFT is transformed into an array of absolute magnitudes and returned to the plotting subroutine for display. Upon completion of the plot, the program ends.

USER'S GUIDE

NOTE: This computer program has been designed for execution on the INTERDATA M70/M80 computers of the M.I.T. Joint Mechanical/Civil Engineering Computer Facility exclusively. Alterations will be required to fulfill the conditions of plotting and Fourier transform subroutines at other facilities.

The computer program is virtually self-contained requiring only two cards for execution per computer run once the parameter value cards have been installed. These cards provide the nomenclature for the 'x' and 'y' axes of the plotting subroutine. These cards are placed into the card deck as shown below in the following order: platform displacement vs. τ ; absolute value of platform displacement vs. ω . The format of these two data cards is 2A40.

The platform/conductor system parameters are included in the program main body. Each parameter may be varied individually by changing the appropriate card value.

The program execution is controlled by submitting the card deck as follows:

```
// JOB
// FOR
PROGRAM DECK (including subroutines)
RETURN
END
// XEQ2
*EL FFTS
*BC 2866
DATA CARDS (TWO)
// END
```

The following pages list the program and an example output.

COMPLEX PWR(512),WTAB(256)

INTEGER*2 XLAB(40)

EXTERNAL AREA

DIMENSION GAP1BR(512),GAP2BR(512),A(2,512),XSCL(4)

COMMON R1(512),R2(512),C1(512),C2(512),TAU(512),PI,AMU,GAMMA1,PSI,
2RHO,R1K0,R1K1,R1K2,R1K3,C1K0,C1K1,C1K2,C1K3,R2K0,R2K1,R2K2,R2K3,
3C2K0,C2K1,C2K2,C2K3,L,DAMCO1,DELTAU,F01

C SET INITIAL VALUES FOR ARRAYS AND PARAMETERS

DO 1 I= 1,512

R1(I) = 0.0

R2(I) = 0.0

C1(I) = 0.0

C2(I) = 0.0

GAP1BR(I) = 0.0

GAP2BR(I) = 0.0

A(1,I) = 0.0

A(2,I) = 0.0

1 TAU(I) = 0.0

DAMCO1 = 0.03

L = 0

PI = 3.14159625

GAMMA1 = 1.0

DO = 19.5

DELTAU = .1

F01 = .01

F0 = 79984.

A-6

AK1 = 90784.

DI = 17.2

RHO = .01

PSI = .0099998

AMU = .1

J = 0

DBAR = (D0 - DI)/(F0/AK1)

GAP1BR(1) = 0.0

GAP2BR(1) = DBAR

WRITE(5,30)

30 FORMAT(T10,'TIME',T24,'PLATFORM DISP',T43,'PLATFORM VEL',T60,'COND
DUCTOR DISP',T80,'CONDUCTOR VEL',T99,'GAP1 BAR',//)

C START THE PROBLEM BY INTEGRATING WITH A 4TH ORDER RUNGA-KUTTA APPR

N = 1

4 DO=3111= N,511

L(I) =

J = I + 1

TAU(J) = TAU(I) + DELTAU

A(2,J) = TAU(J)

CALL RK0

CALL RK1

CALL RK2

CALL RK3

R1(J) = AREA (R1(I),DELTAU,R1K0,R1K1,R1K2,R1K3)

A(1,J) = R1(J)

R2(J) = AREA (R2(I),DELTAU,R2K0, R2K1,R2K2,R2K3)

A-7

```
C1(J) = AREA (C1(I),DELTAU,C1K0,C1K1,C1K2,C1K3)
C2(J) = AREA ( C2(I),DELTAU,C2K0,C2K1,C2K2,C2K3)

C   CHECK THE GAP DISTANCES BETWEEN THE PLATFORM AND THE CONDUCTOR

GAP1BR(J) = GAP1BR(I) +(C1(J) - C1(I)) - (R1(J) - R1(I))
GAP2BR(J) = DBAR - GAP1BR(J)

IF(GAP1BR(J) .LT. 0.0) GO TO 600
700 IF(GAP1BR(J) .EQ. 0.0) GO TO 100
    IF(GAP2BR(J) .LT. 0.0) GO TO 800
900 IF(GAP2BR(J) .EQ. 0.0) GO TO 100
    3 CONTINUE
100 IF( J .EQ. 512) GO TO 400

C   WHEN A GAP GOES TO 0.0, CONSERVE MOMENTUM

N = L + 1

WRITE(5,40) TAU(N)
40 FORMAT(/,T6,'CONTACT OCCURRED AT TIME,',2X,1PE12.4,/)

IF(GAP1BR(N) .EQ. 0.0) GAP2BR(N) = DBAR
IF(GAP2BR(N) .EQ. 0.0) GAP1BR(N) = DBAR
R2(N) =(1./(1. +AMU)) * R2(N)
C2(N) = R2(N)

C   INTEGRATE THE SYSTEM WITH COMBINED MASSES

DO 5 I= N,511

C   CHECK THE CONTACT FORCE BEFORE INTEGRATION TO ENSURE NO SEPARATION

FI = 2.* PI * GAMMA1 * TAU(I)

C   ACCEL IS A DUMMY VARIABLE FOR THE ACCELERATION AT ANY TIME TAU

ACCEL = (4. * PI/(1. + AMU)) * (PI * SIN(FI)-DAMCO1 * R2(I) - PS
2I * DAMCO1 * R2(I) - PI * RHO * C1(I))
```

```

C      FHat IS THE VARIABLE FOR THE CONTACT FORCE

      FHat = F01 * PSI * DAMCO1 * R2(I)/PI + RHO * F01 * C1(I) - AMU *
2F01 * ACCEL/ (4. * PI**2)

      IF( FHat .EQ. 0.0) GO TO 15
      IF( FHat .LT. 0.0) GO TO 15

      L = I
      J = L + 1

      TAU(J) = TAU(I) + DELTAU
      A(2,J) = TAU(J)

      CALL RK01
      CALL RL11
      CALL RK21
      CALL RK31

      R1(J) = AREA (R1(I),DELTAU,R1K0,R1K1,R1K2,R1K3)
      A(1,J) = R1(J)

      R2(J) = AREA (R2(I),DELTAU,R2K0,R2K1,R2K2,R2K3)
      C1(J) = C1(I) +(R1(J) - R1(I))
      C2(J) = R2(J)

      GAP1BR(J) = GAP1BR(I)
      GAP2BR(J) = GAP2BR(I)

      GO TO 20

15 WRITE(5,25) TAU(I),R1(I),R2(I),C1(I),C2(I),GAP1BR(I)
25 FORMAT(T6,1PE12.4,T25,1PE12.4,T43,1PE12.4,T61,1PE12.4,T81,1PE12.4,
2T97,1PE12.4)

      IF(J .EQ. 512) GO TO 400

```


A-9

```
WRITE(5,11) TAU(J)

11 FORMAT(/,T6,'THE CONTACT FORCE IS ZERO;MASS SEPARATION OCCURRED
2AT TIME,'2X,1PE12.4,/)

N = L + 1

GO TO 4

20 WRITE(5,10) TAU(J),R1(J),R2(J),C1(J),C2(J),GAP1BR(J)

10 FORMAT(T6,1PE12.4,T25,1PE12.4,T43,1PE12.4,T61,1PE12.4,T81,1PE12.4,
2T97,1PE12.4)

5 CONTINUE

40C M = 0

GO TO 53

54 DO 50 I = 1,512

50 PWR(I) = CMPLX(R1(I),0.0)

NBITS = 9

NEWTB = 1

INV = 1

CALL FFT (PWR,NBITS,INV,WTAB,NEWTB)

C THE VARIABLE 'S' IS THE INCREMENTAL FREQUENCY OVER WHICH THE
C FOURIER TRANSFORM WILL BE PLOTTED, AND THE CONSTANT IN THE 'S'
C EQUATION IS EQUAL TO '2*PI/(512.*DELTAU) '

S = 0.0

DO 51 I = 1,512

A(1,I) = CABS(PWR(I))

A(2,I) = S

51 S = S + .6136

53 NROW = 2
```

A-10

```
XSCL(1) = 0.0
XSCL(2) = 0.0
XSCL(3) = 0.0
XSCL(4) = 0.0
NVAR = 1
NPTS = 512
NX = 2
MOVE = 0
LABEL = 4
ISCL = 1
FTIME = 0.0
LOOK = 1
READ(8,45) (XLAB(I), I = 1,40)
45 FORMAT (40A2)
CALL PICTR(A,NROW,XLAB,XSCL,NVAR,NPTS,NX,MOVE,LABEL,ISCL,FTIME,
2LOOK)
M = M + 1
IF(M .EQ. 1) GO TO 54
GO TO 35
600 GAP1BR(J) = 0.0
GAP2BR(J) = DBAR
C1(J) = R1(J)
GO TO 700
800 GAP2BR(J) = 0.0
GAP1BR(J) = DBAR
C1(J) = R1(J) + DBAR
```

A-11

GO TO 900

35 STOP

END

A-12

C THE RK0 SUBROUTINE DETERMINES THE K1 COEFFICIENTS DURING
C COMPONENT SEPARATION

SUBROUTINE RK0

COMMON R1(512),R2(512),C1(512),C2(512),TAU(512),PI,AMU,GAMMA1,PSI,
2RHO,R1K0,R1K1,R1K2,R1K3,C1K0,C1K1,C1K2,C1K3,R2K0,R2K1,R2K2,R2K3,
3C2K0,C2K1,C2K2,C2K3,L,DAMCO1,F01, DELTAU

PI2 = PI **2

FI = 2.*PI * GAMMA1 * TAU(L)

R1K0 = R2(L)

R2K0 = (4. *PI2) * (SIN(FI) - R1(L)) - 4. * PI * DAMCO1 * R2(L)

C1K0 = C2(L)

C2K0 = -(4. * PI * PSI * DAMCO1 * C2(L)/AMU) - (PI2 * 4. * RHO *
2C1(L)/AMU)

RETURN

END

C THE RK1 SUBROUTINE DETERMINES THE K2 COEFFICIENTS DURING
C COMPONENT SEPARATION

SUBROUTINE RK1

COMMON R1(512),R2(512),C1(512),C2(512),TAU(512),PI AMU,GAMMA1,PSI,
2RHO,R1K0,R1K1,R1K2,R1K3,C1K0,C1K1,C1K2,C1K3,R2K0,R2K1,R2K2,R2K3,
3C2K0,C2K1,C2K2,C2K3,L,DAMCO1,F01,DELTAU

PI2 = PI **2

B = DELTAU / 2.

T = TAU(L) + B

E1 = R1(L) + B * R1K0

E2 = R2(L) + B * R2K0

E3 = C1(L) + B * C1K0

E4 = C2(L) + B * C2K0

FI = 2. * PI * GAMMA1 * T

R1K1 = E2

R2K1 = (4. * PI2) * (SIN(FI) - E1) - 4. * PI * DAMCO1 * E2

C1K1 = E4

C2K1 = -(4. * PI*PSI*DAMCO1*E4/AMU) - (PI2 * 4.*RHO*E3/AMU)

RETURN

END

C THE RK2 SUBROUTINE DETERMINES THE K3 COEFFICIENTS DURING
C COMPONENT SEPARATION

SUBROUTINE RK2

COMMON R1(512),R2(512),C1(512),C2(512),TAU(512),PI,AMU,GAMMA1,PSI,
2RHO,R1K0,R1K1,R1K2,R1K3,C1K0,C1K1,C1K2,C1K3,R2K0,R2K1,R2K2,R2K3,
3C2K0,C2K1,C2K2,C2K3,L,DAMCO1,DELTAU,F01

B = DELTAU/2.

PI2 = PI **2

T = TAU(L) + B

E1 = R1(L) + B * R1K1

E2 = R2(L) + B * R2K1

E3 = C1(L) + B * C1K1

E4 = C2(L) + B * C2K1

FI = 2. * PI * GAMMA1 * T

R1K2 = E2

R2K2 = (4. * PI2) * (SIN(FI) - E1) - 4. * PI * DAMCO1 * E2

C1K2 = E4

C2K2 = -(4. * PI * PSI * DAMCO1 * E4/AMU) - (PI2 * 4. * RHO * E3/AMU)

RETURN

END

A-15

C THE RK3 SUBROUTINE DETERMINES THE K4 COEFFICIENTS DURING
C COMPONENT SEPARATION

SUBROUTINE RK3

COMMON R1(512),R2(512),C1(512),C2(512),TAU(512),PI,AMU,GAMMA1,PSI,
2RHO,R1K0,R1K1,R1K2,R1K3,C1K0,C1K1,C1K2,C1K3,R2K0,R2K1,R2K2,R2K3,
3C2K0,C2K1,C2K2,C2K3,L,DAMCO1,DELTAU,F01

B = DELTAU

PI2 = PI **2

T = TAU(L) + B

E1 = R1(L) + B * R1K2

E2 = R2(L) + B * R2K2

E3 = C1(L) + B * C1K2

E4 = C2(L) + B * C2K2

FI = 2. * PI * GAMMA1 * T

R1K3 = E2

R2K3 = (4. * PI2) * (SIN(FI) - E1) - 4.*PI*DAMCO1*E2

C1K3 = E4

C2K3 = -(4.*PI*PSI*DAMCO1*E4/AMU) - (PI2* 4.*RHO*E3/AMU)

RETURN

END

A-16

```
C   THE RK01 SUBROUTINE DETERMINES THE K1 COEFFICIENTS FOR THE
C   COMBINED MASSES

SUBROUTINE RK01
COMMON R1(512),R2(512),C1(512),C2(512),TAU(512),PI,AMU,GAMMA1,PSI,
2RHO,R1K0,R1K1,R1K2,R1K3,C1K0,C1K1,C1K2,C1K3,R2K0,R2K1,R2K2,R2K3,
3C2K0,C2K1,C2K2,C2K3,L,DAMCO1,DELTAU,F01

FI = 2. * PI * GAMMA1 * TAU(L)
PI2 = PI **2
R1K0 = R2(L)
R2K0 = (4.*PI/(1.+AMU)) * (PI*SIN(FI)-DAMCO1*R2(L)-PSI*DAMCO1*R2
2(L) - PI * RHO * C1(L))
C1K0 = C1(L)

RETURN

END
```

A-17

C THE RK11 SUBROUTINE DETERMINES THE K2 COEFFICIENTS FOR THE
C COMBINED MASSES

SUBROUTINE RK11

COMMON R1(512),R2(512),C1(512),C2(512),TAU(512),PI,AMU,GAMMA1,PSI,
2RHO,R1K0,R1K1,R1K2,R1K3,C1K0,C1K1,C1K2,C1K3,R2K0,R2K1,R2K2,R2K3,
3C2K0,C2K1,C2K2,C2K3,L,DAMCO1,DELTAU,F01

B = DELTAU + B

T = TAU(L) + B

FI = 2. * PI * GAMMA1 * T

E1 = R1(L) + B * R1K0

E2 = R2(L) + B * R2K0

E3 = C1(L) + B * C1K0

R1K1 = E2

R2K1 = (4. * PI/(1.+ AMU))*(PI*SIN(FI) -DAMCO1*E2/PSI*DAMCO1*E2

2-PI * RHO * E3)

C1K1 = E3

RETURN

END

C THE RK21 SUBROUTINE DETERMINES THE K3 COEFFICIENTS FOR THE

C COMBINED MASSES

SUBROUTINE RK21

COMMON R1(512),R2(512),C1(512),C2(512),TAU(512),PI,AMU,GAMMA1,PSI,
2RHO,R1K0,R1K1,R1K2,R1K3,C1K0,C1K1,C1K2,C1K3,R2K0,R1K1,R2K2,R2K3,
3C2K0,C2K1,C2K2,C2K3,L,DAMCO1,DELTAU,F01

B = DELTAU / 2.

T = TAU(L) + B

FI = 2. * PI * GAMMA1 * T

E1 = R1(L) + B * R1K1

E2 = R2(L) + B * R2K1

E3 = C1(L) + B * C1K1

R1K2 = E2

R2K2 = (4. * PI / (1. + AMU)) * (PI * SIN(FI) - DAMCO1 * E2 - PSI * DAMCO1 * E2 - PI * E1 -

2PI * RHO * E3)

C1K2 = E3

RETURN

END

C THE RK31 SUBROUTINE DETERMINES THE K4 COEFFICIENTS FOR THE
C COMBINED MASSES

SUBROUTINE RK31

COMMON R1(512), R2(512), C1(512), C2(512), TAU(512), PI, AMU, GAMMA1, PSI,
2RHO, R1K0, R1K1, R1K2, R1K3, C1K0, C1K1, C1K2, C1K3, R2K0, R2K1, R2K2, R2K3,
3C2K0, C2K1, C2K2, C2K3, L, DAMC01, DELTAU, F01

B = DELTAU

T = TAU(L) + B

FI = 2. * PI * GAMMA1 * T

E1 = R1(L) + B * R1K2

E2 = R2(L) + B * R2K2

E3 = C1(L) + B * C1K2

R1K3 = E2

R2K3 = (4. * PI / (1. + AMU)) * (PI * SIN(FI) - DAMC01 * E2 - PSI * DAMC01 * E2 - PI *

2RHO * E3)

C1K3 = E3

RETURN

END

A-20

C THE AREA FUNCTION COMPUTES: $Y(N+1) - Y(N)$ FOR R1,R2,C1,C2

FUNCTION AREA(B1,B2,B3,B4,B5,B6)

AREA = $B1 + B2/6. * (B3 + 2.*B4 + 2.*B5 + B6)$

RETURN

END

TIME	PLATFORM DISP	PLATFORM VEL	CONDUCTOR DISP	CONDUCTOR VEL	GAP1 BAR
1.0000E-01	2.0392E-02	5.8704E-01	0.0000E 00	0.0000E 00	-2.0392E-02
CONTACT OCCURRED AT TIME, 1.0000E-01					
1.0000E-01	2.0392E-02	5.3367E-01	2.0392E-02	5.3367E-01	0.0000E 00
THE CONTACT FORCE IS ZERO; MASS SEPARATION OCCURRED AT TIME, 1.0000E-01					
2.0000E-01	1.4261E-01	1.9984E 00	7.2908E-02	5.1321E-01	-6.9700E-02
CONTACT OCCURRED AT TIME, 2.0000E-01					
2.0000E-01	1.4261E-01	1.8167E 00	1.4261E-01	1.8167E 00	0.0000E 00
THE CONTACT FORCE IS ZERO; MASS SEPARATION OCCURRED AT TIME, 2.0000E-01					
3.0000E-01	4.0861E-01	3.4611E 00	3.1994E-01	1.7184E 00	-8.8671E-02
CONTACT OCCURRED AT TIME, 3.0000E-01					
3.0000E-01	4.0861E-01	3.1465E 00	4.0861E-01	3.1465E 00	0.0000E 00
THE CONTACT FORCE IS ZERO; MASS SEPARATION OCCURRED AT TIME, 3.0000E-01					
4.0000E-01	7.8323E-01	4.1886E 00	7.1257E-01	2.9129E 00	-7.0658E-02
CONTACT OCCURRED AT TIME, 4.0000E-01					
4.0000E-01	7.8323E-01	3.8079E 00	7.8323E-01	3.8079E 00	0.0000E 00
THE CONTACT FORCE IS ZERO; MASS SEPARATION OCCURRED AT TIME, 4.0000E-01					
5.0000E-01	1.1687E 00	3.6882E 00	1.1454E 00	3.4122E 00	-2.3337E-02

CONTACT OCCURRED AT TIME, 5.0000E-01

5.0000E-01	1.1687E 00	3.3529E 00	1.1687E 00	3.3529E 00	0.0000E 00
------------	------------	------------	------------	------------	------------

THE CONTACT FORCE IS ZERO; MASS SEPARATION OCCURRED AT TIME, 5.0000E-01

6.0000E-01	1.4427E 00	1.9320E 00	1.4782E 00	2.8170E 00	3.5492E-02
7.0000E-01	1.5194E 00	-5.1925E-01	1.7285E 00	2.1725E 00	2.0911E-01
8.0000E-01	1.3246E 00	-3.3702E 00	1.9100E 00	1.4450E 00	5.8531E-01
9.0000E-01	8.5935E-01	-5.7973E 00	2.0157E 00	6.6358E-01	1.1563E 00
1.0000E 00	2.0425E-01	-7.0740E 00	2.0419E 00	-1.4098E-01	1.8376E 00
1.1000E 00	-5.0320E-01	-6.8228E 00	1.9878E 00	-9.3698E-01	2.4910E 00
1.2000E 00	-1.1110E 00	-5.1375E 00	1.8558E 00	-1.6932E 00	2.9669E 00

CONTACT OCCURRED AT TIME, 1.2000E 00

1.3000E 00	-1.6652E 00	-6.5619E 00	9.4535E-01	-6.5619E 00	2.6106E 00
1.4000E 00	-2.4519E 00	-9.2838E 00	1.5866E-01	-9.2838E 00	2.6106E 00
1.5000E 00	-3.5624E 00	-1.3001E 01	-9.5187E-01	-1.3001E 01	2.6106E 00
1.6000E 00	-5.1228E 00	-1.8250E 01	-2.5122E 00	-1.8250E 01	2.6106E 00
1.7000E 00	-7.3663E 00	-2.6649E 01	-4.7557E 00	-2.6649E 01	2.6106E 00

THE CONTACT FORCE IS ZERO; MASS SEPARATION OCCURRED AT TIME, 1.7000E 00

1.8000E 00	-8.5606E 00	3.4232E 00	-7.3046E 00	-2.4164E 01	1.2559E 00
1.9000E 00	-6.7269E 00	3.2029E 01	-9.5571E 00	-2.0740E 01	-2.8302E 00

CONTACT OCCURRED AT TIME, 1.9000E 00

APPENDIX B

In this appendix the individual platform system responses are presented. Each plot is serialized below the abscissa in a statement, "Run Code XYZ." The code is interpreted as follows: X = 1; the plot is the result of a R-K integration.

Y = 1 through 7; denotes the value of γ_1 used in the R-K integration.

Z = 1 through 3; denotes the value of F01 used during the R-K integration.

A complete description of the codes is listed in Table B.1.

TABLE B.1, Computer Run Code Summary

CODE	γ_1	F01	CODE	γ_1	F01
111	0.5	0.01	152	2.0	0.001
121	0.8	0.01	162	3.0	0.001
131	1.0	0.01	172	5.0	0.001
141	1.5	0.01	113	0.5	0.0001
151	2.0	0.01	123	0.8	0.0001
161	3.0	0.01	133	1.0	0.0001
171	5.0	0.01	143	1.5	0.0001
112	0.5	0.001	153	2.0	0.0001
122	0.8	0.001	163	3.0	0.0001
132	1.0	0.001	173	5.0	0.0001
142	2.0	0.001			

Each plot is followed by an analysis of the platform response with respect to steady-state magnitude, the effect of the excitation frequency, the position of the dynamic equilibrium, positive or negative, relative to the static equilibrium zero position and the primary response frequencies as determined by a Fourier transform of the platform response. The plots which were computed for $F01$ equal to 0.0001 are included without an explanation of the plots. These plots coincided with the platform response plots for $F01$ equal to 0.001 for all values of γ_1 . Therefore no additional information could be obtained from them.

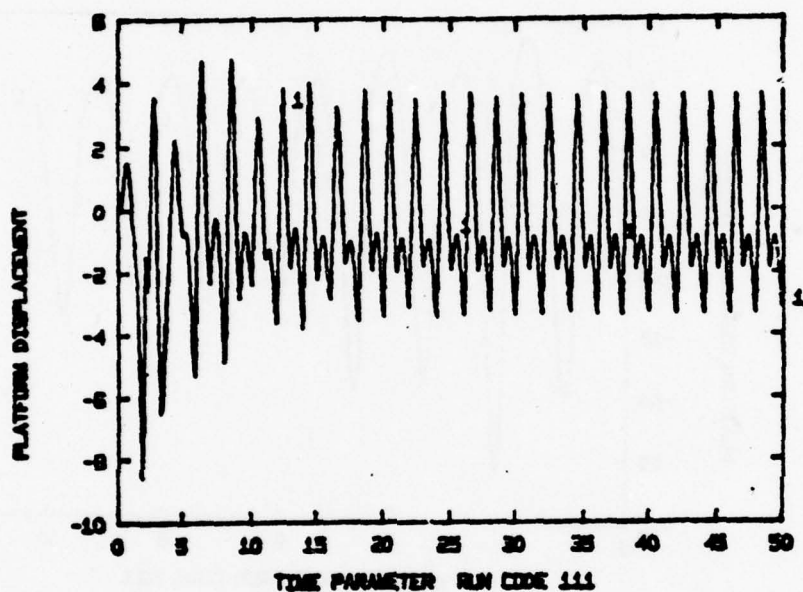


FIGURE B.1, Platform Response for $F_{01} = 0.01$; $\gamma_1 = 0.5$

The steady-state platform displacement is 3.5 units. The period between maximum displacements is 2π which corresponds to the excitation frequency of 1 radian/second. The dynamic equilibrium position is slightly positive. The Fourier transform of the platform response yields primary frequencies of 0.42 and 0.84 radians/second. These frequencies correspond to the difference between the excitation frequency and the conductor natural frequency, and the first harmonic of this frequency.

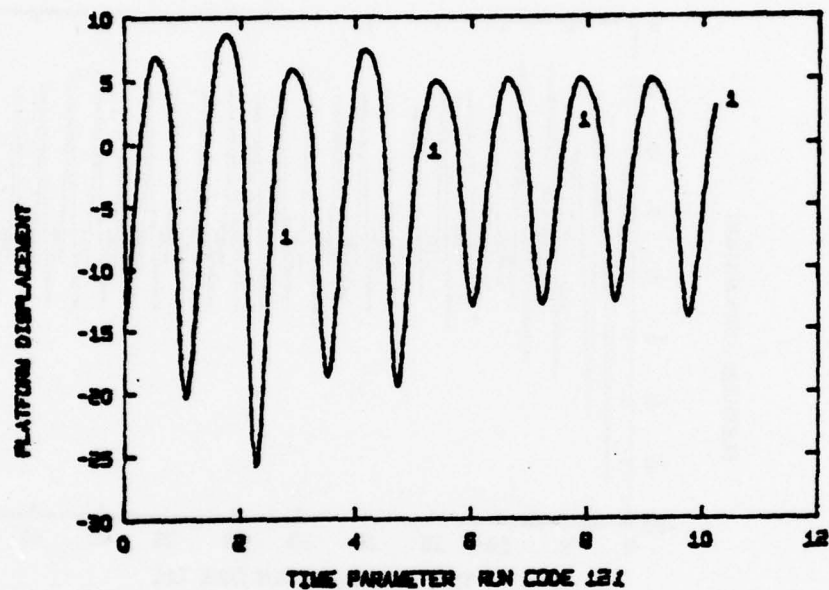


FIGURE B.2, Platform Response for $F_{01} = 0.01$; $\gamma_1 = 0.8$

The steady-state magnitude of the platform response is 8.87 units. The period of the response is 1.25π corresponding to the excitation frequency. The dynamic equilibrium position is 3.84 units negative. The primary frequencies of the response are the excitation frequency, the sum of the excitation frequency and the platform natural frequency, and an unidentified combination of frequencies equal to 5.7 radians/second. More comprehensive data is required to determine the exact components of this frequency.

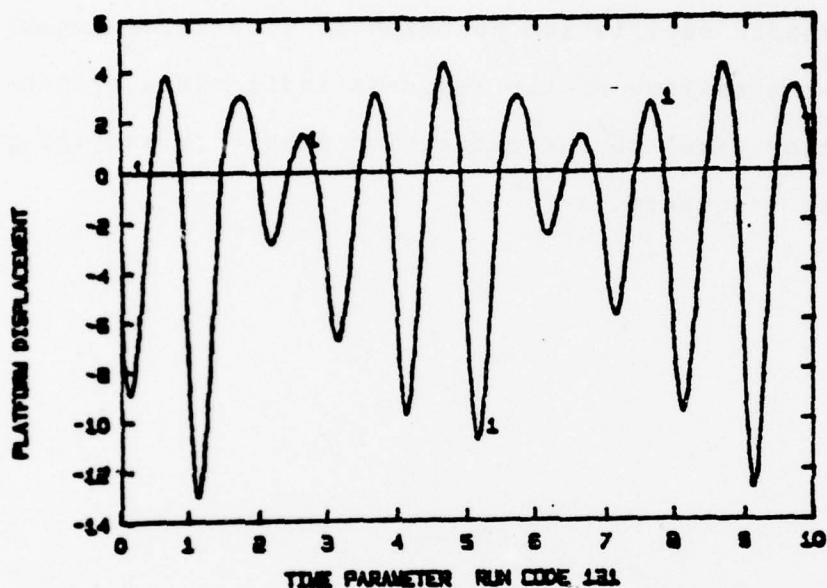


FIGURE B.3, Platform Response for $F_{01} = 0.01$; $\gamma_1 = 1.0$

The average steady-state response magnitude is 5.19 units. The frequency of the displacement is equal to the excitation frequency. As the overall displacement moves in the negative direction, the individual cycle amplitudes increase over a four cycle period such that if the equilibrium position were normalized, a beat frequency would be prevalent. If this conclusion is true, the period over the four cycles should be equal to one-half the beat frequency period, or $2\pi/(\omega_1 - \omega_2)$. Substituting the natural frequencies of the platform and

the conductor for ω_1 and ω_2 respectively, the period is 4.28τ . By inspection of the displacement plot, the period of the four cycles is approximately 4τ . Thus, a beat frequency caused by the interaction of the platform and the conductor is a plausible explanation of the platform displacement plot. The dynamic equilibrium position is 2.36 units negative. The Fourier transform of the response indicates a primary frequency equal to the excitation frequency and the platform natural frequency.

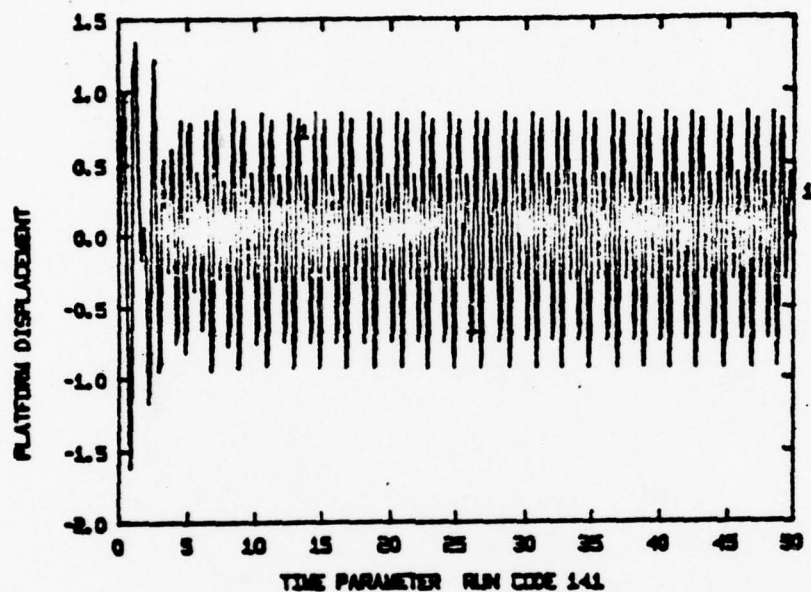


FIGURE B.4, Platform Response for $F_{01} = 0.01$; $\gamma_1 = 1.5$

The steady-state response magnitude is 0.67 units. The period over one response cycle is 0.66τ corresponding to the excitation frequency. However, the period between two adjacent peaks of equal amplitude is 2τ . The dynamic equilibrium position is slightly positive. From the Fourier transform of the response, the principle frequencies are the excitation frequency, the platform natural frequency and a frequency equal to the difference between these two frequencies. The period of the third frequency is 2τ corresponding to the predominant

B-8

period between displacement peaks.

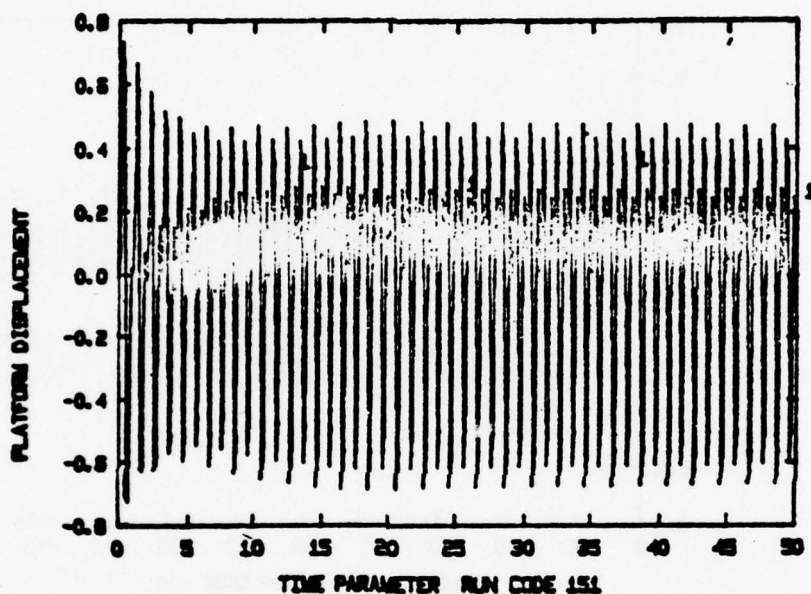


FIGURE B.5, Platform Response for $F_{01} = 0.01$; $\gamma_1 = 2.0$

The steady-state response magnitude is 0.50 units. The platform oscillates alternately with a period which equates to the sum of the platform and conductor natural frequencies and a period which is twice the summation frequency. The variation in response period implies that the platform and conductor are alternately in and out-of-phase. The dynamic is slightly positive. The Fourier transform indicates primary frequencies equal to the excitation frequency and the platform natural frequency.

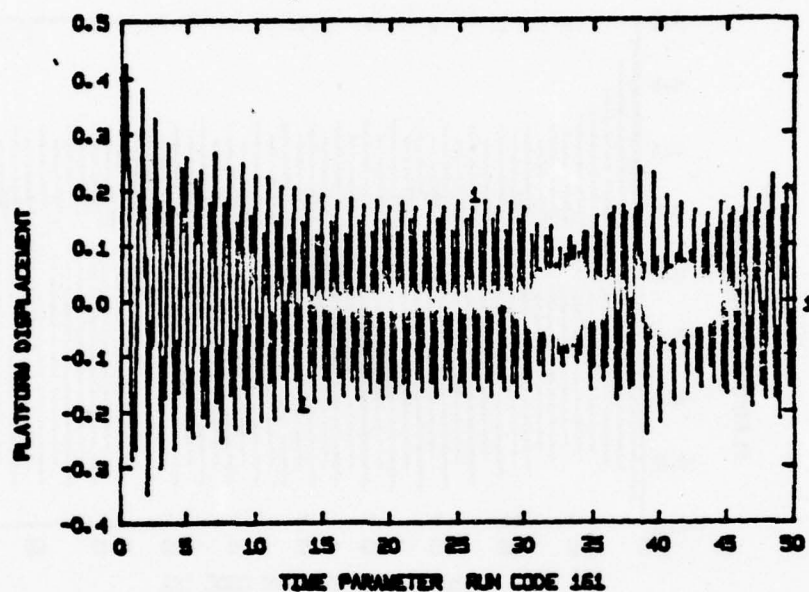


FIGURE B.6, Platform Response for $F_{01} = 0.01$; $\gamma_1 = 3.0$

The average steady-state magnitude is 0.2 units. In steady-state, the platform response has a beat frequency superimposed. The beat period is 20τ which is a frequency of 0.1 radians/second. The dynamic equilibrium position is slightly positive. The primary response frequencies are the excitation frequency and the platform natural frequency.

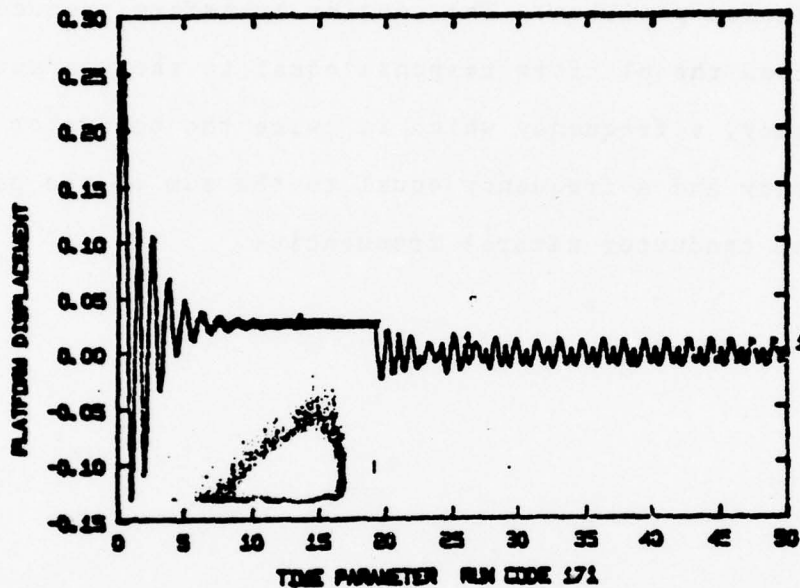


FIGURE B.7, Platform Response for $F_{01} = 0.01$; $\gamma_1 = 5.0$

The steady-state magnitude is 0.012 units. Uniquely, the system settled into an unstable equilibrium position before reaching its final, steady-state equilibrium position. The system cycles at a frequency of 2.65 radians/second which equates approximately to the sum of the platform and the conductor natural frequencies. It appears that at this high excitation frequency the relative velocities of the conductor are at a level such that the platform and conductor momenta are nearly equal. When the conductor and platform

are out-of-phase, the momentum of the conductor is sufficient enough to cancel the momentum of the platform causing a reduction in platform motion. When the two components are in phase, the platform displacement nearly doubles. The dynamic equilibrium position coincides with the static equilibrium position. The fourier transform produces frequencies from the platform response equal to the conductor natural frequency, a frequency which is twice the conductor natural frequency and a frequency equal to the sum of the platform and the conductor natural frequencies.

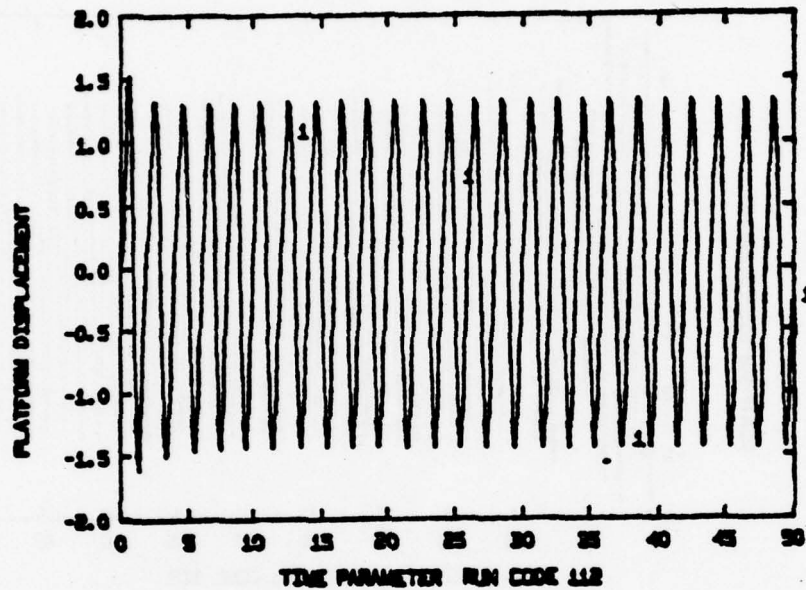


FIGURE B.8, Platform Response for $F_{01} = 0.001$; $\gamma_1 = 0.5$

The steady-state magnitude is 1.35 units. The period of the response is 2π which equates to the excitation frequency. The dynamic equilibrium position is slightly negative. From the Fourier transform, the primary response frequencies are the excitation frequency and the platform natural frequency.

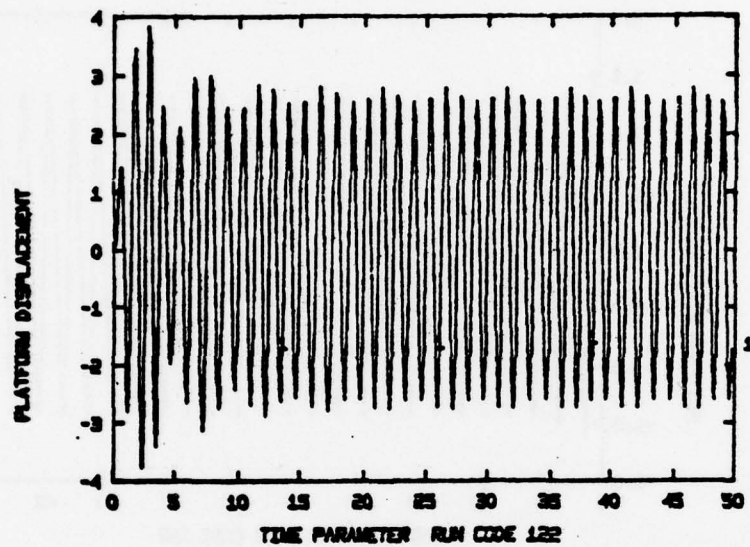


FIGURE B.9, Platform Response for $F_0 = 0.001$; $\gamma_1 = 0.3$

The average steady-state magnitude is 2.6 units. The individual displacement cycles have a period of 1.25τ which is the excitation frequency. There is a slight beat frequency superimposed which has a period of 10τ and a frequency of 0.2 radians/second. The dynamic equilibrium position is slightly positive. The Fourier transform yields primary frequencies equal to the excitation frequency and the platform natural frequency from the platform response.

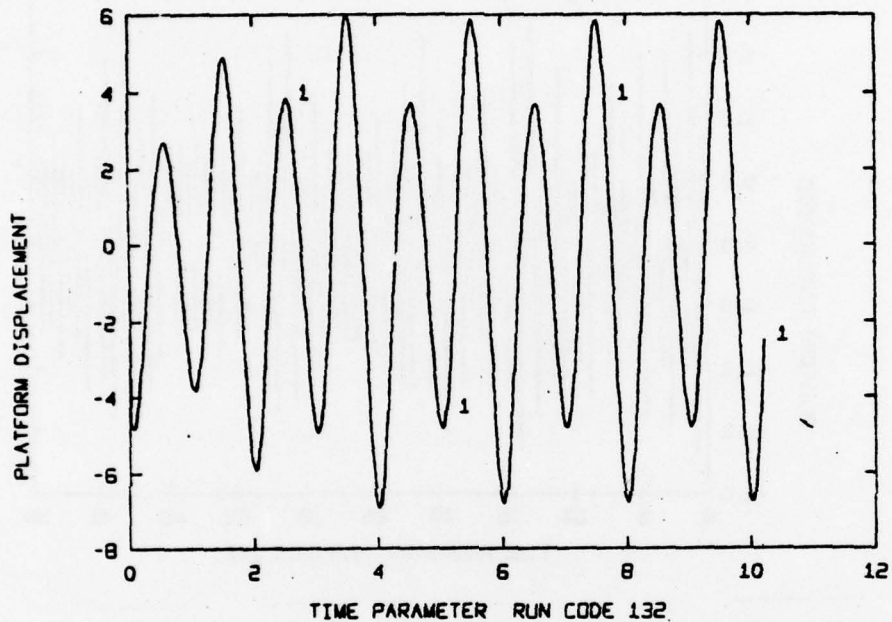


FIGURE B.10, Platform Response for $F_{01} = 0.001$; $\gamma_1 = 1.0$

The average steady-state magnitude is 5.3 units. The platform displacement period is 1τ corresponding to the excitation frequency and the platform natural frequency. A beat frequency is more prominent. The beat period is 4τ which is a frequency of 0.52 radians/second. The dynamic equilibrium position is 0.55 units negative. From the Fourier transform, the primary frequency is the excitation frequency. Nothing in the transform indicates the component frequencies which make up the beat frequency.

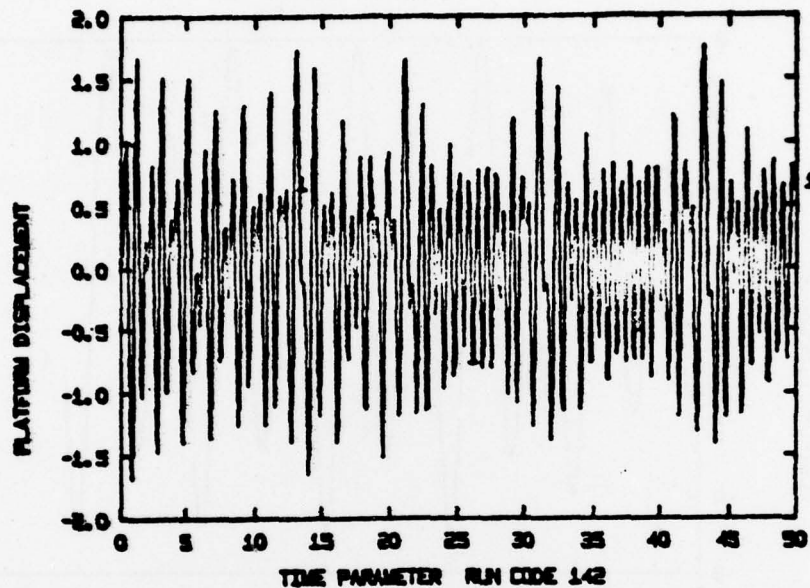


FIGURE B.11, Platform Response for $F_{01} = 0.001$; $\gamma_1 = 1.5$

The average steady-state magnitude is 1.1 units. The period of a displacement cycle is 0.67τ which equates to the excitation frequency. The beat phenomena has a period of 24τ and a frequency of 0.08 radians/second. The dynamic equilibrium position is 0.07 units positive. The Fourier transform of the platform response indicates primary frequencies equal to the excitation frequency, the platform natural frequency and a frequency of 1.87 radians/second which requires further analysis for component identification.

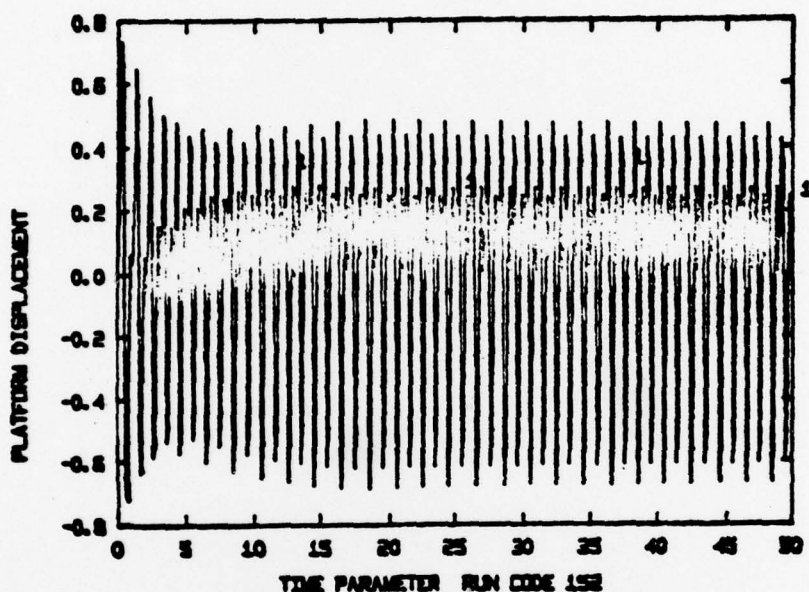


FIGURE B.12, Platform Response for $F_{01} = 0.001$; $\gamma_1 = 2.0$

The steady-state displacement magnitude is 0.50 units. The period of the response cycle cannot be uniquely determined as the period varies over adjacent cycles as the displacement amplitude alternately increases and decreases. However, over four cycles the average period is 0.5π which corresponds to the excitation frequency. The period of the amplitude alteration is 4π which is a frequency of 0.53 radians/second. The dynamic equilibrium position is negative slightly. The Fourier transform of the response indicates primary frequen-

B-18

cies equal to the excitation frequency and the platform natural frequency.

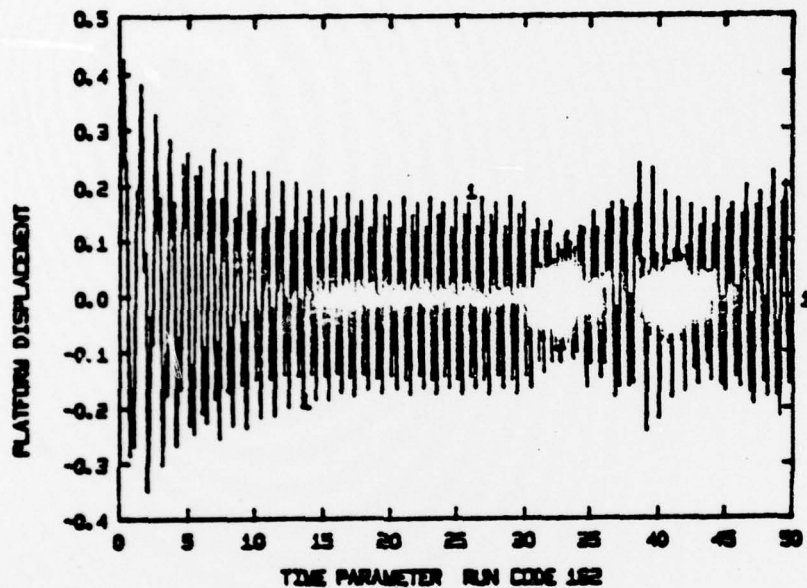


FIGURE B.13, Platform Response for $F_{01} = 0.001$; $\gamma_1 = 3.0$

The average steady-state magnitude is 0.2 units. The displacement period is 0.33τ which is the excitation frequency. The platform response exhibits a beat phenomena with a period of 24τ and a frequency of 0.08 radians/second. The dynamic equilibrium position is slightly positive. From the Fourier transform of the response, the primary frequencies are the excitation frequency and the platform natural frequency. It appears that the excitation frequency is sufficiently removed from the platform natural frequency that excitation force

B-20

is an insignificant factor. This response plot duplicates the response plot for F01 equal to 0.01.

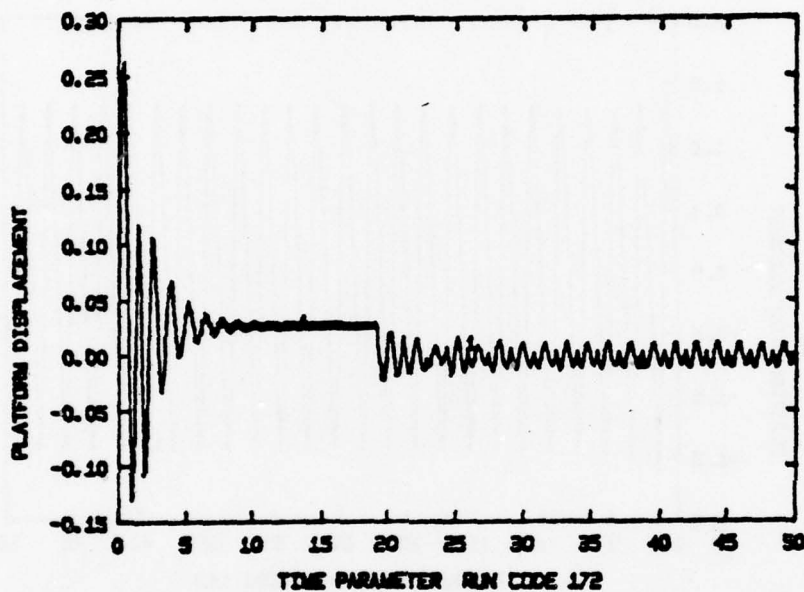


FIGURE B.14, Platform Response for $F_{01} = 0.001$; $\gamma_1 = 5.0$

This platform response plot coincides exactly with the plot for F_{01} equal to 0.01. The steady-state magnitude is 0.012 units. The dynamic equilibrium position coincides with the static equilibrium position. The primary frequencies from the Fourier transform of the response are the sum of the platform and conductor natural frequencies, the conductor natural frequency and a frequency which is twice the conductor natural frequency.

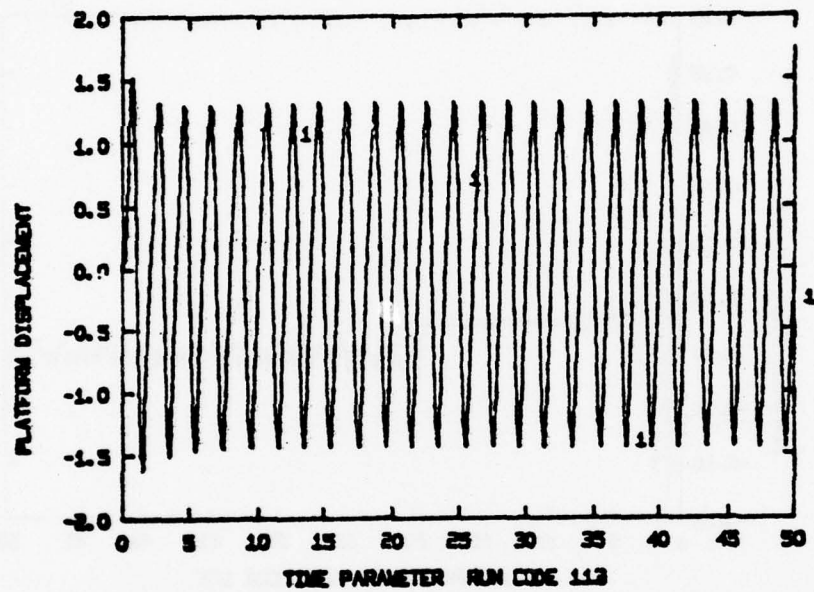


FIGURE B.15, Platform Response for $F_{01} = 0.0001$; $\gamma_1 = 0.5$

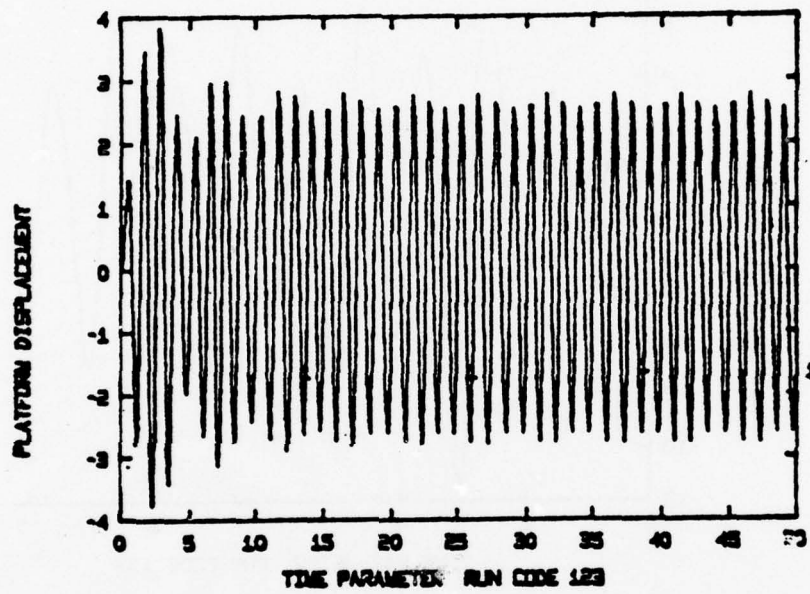


FIGURE B.16, Platform Response for $F_{01} = 0.0001$; $\gamma_1 = 0.8$

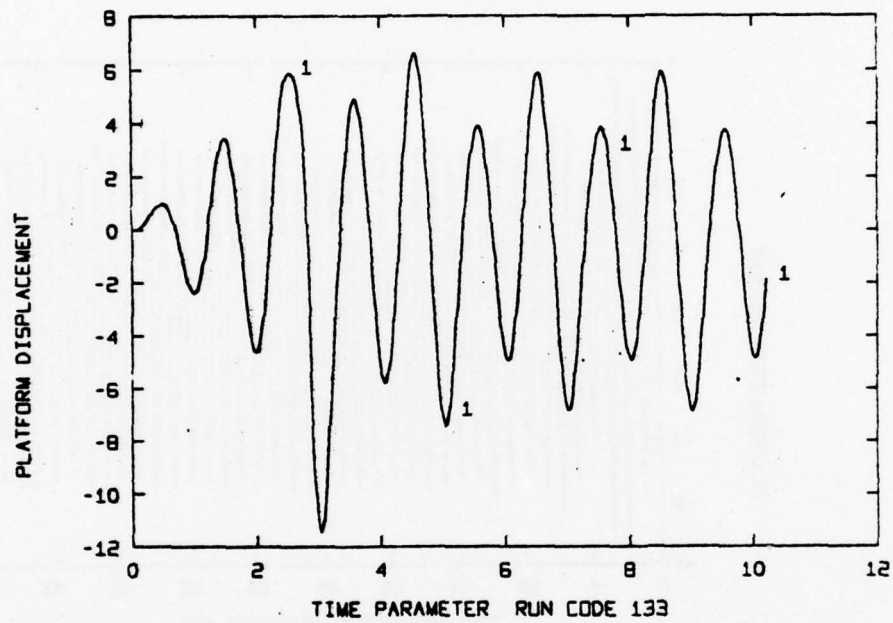


FIGURE B.17, Platform Response for $F_{01} = 0.0001$; $\gamma_1 = 1.0$

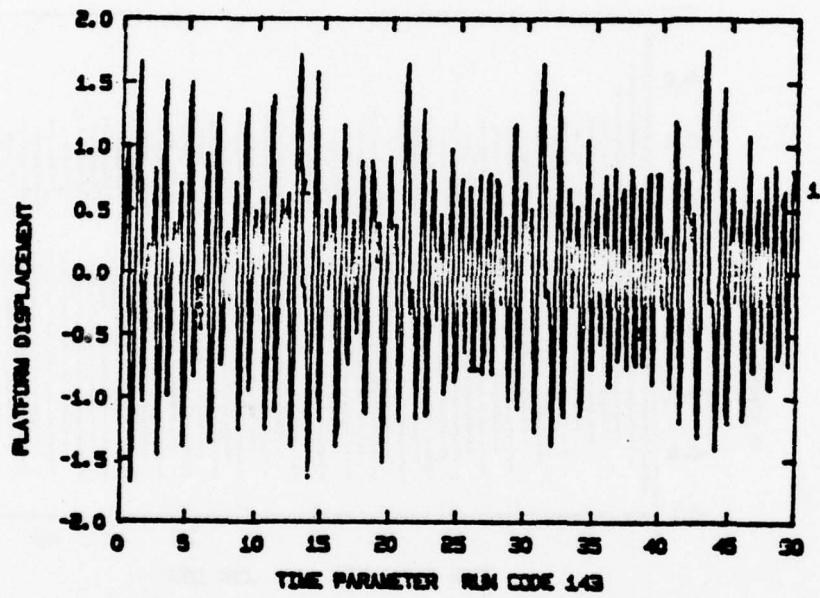


FIGURE B.18, Platform Response for $F_{01} = 0.0001$; $\gamma_1 = 1.5$

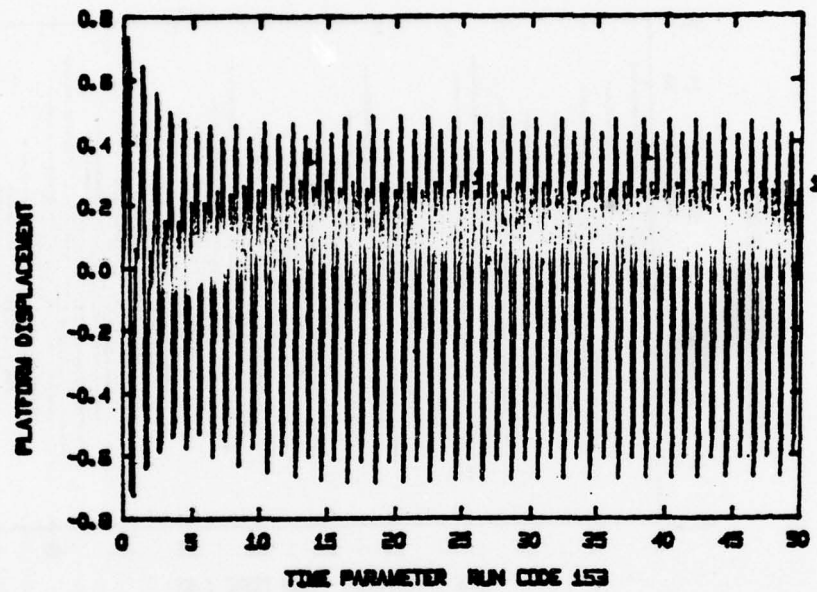


FIGURE B.19, Platform Response for $F_{01} = 0.0001$; $\gamma_1 = 2.0$

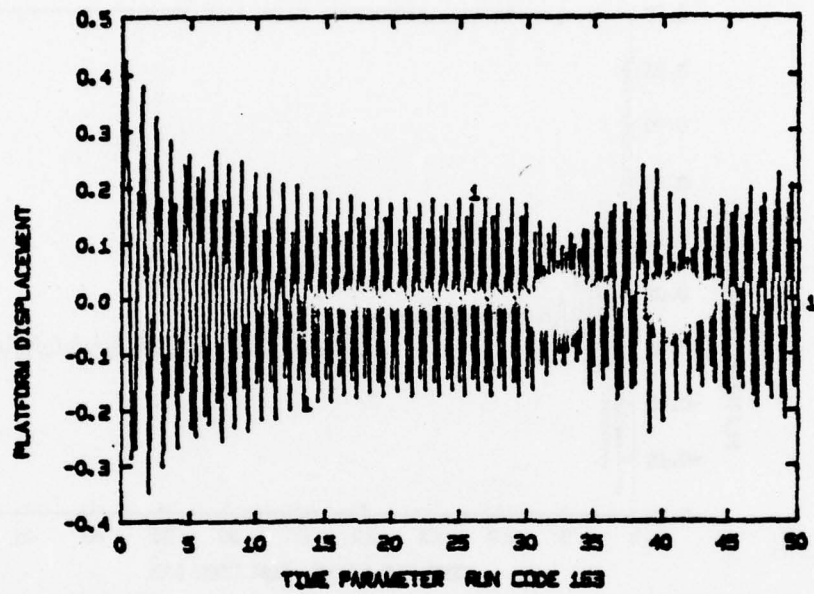


FIGURE B.20, Platform Response for $F_{01} = 0.0001$; $\gamma_1 = 3.0$

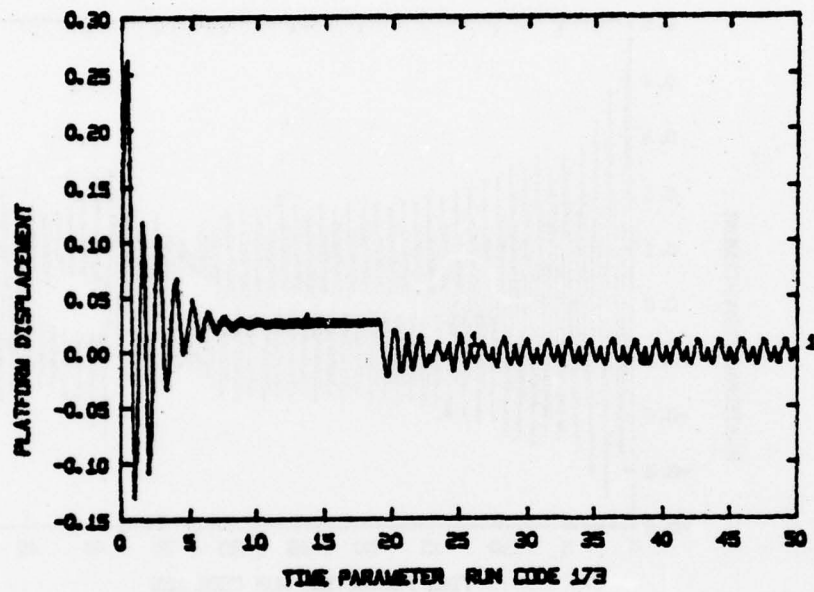


FIGURE B.21, Platform Response for $F_0 = 0.0001$; $\gamma_1 = 5.0$